

Department of Clinical Microbiology
Clinical Institute of Laboratory Medicine
Medical University of Vienna

(Head: Ao. Univ. Prof.ⁱⁿ Dr.ⁱⁿ med. Birgit Willinger)

**Emergence of Terbinafine and Azole Resistance in Dermatophytes:
Prevalence in Austria and Resistance Mechanisms**

Master Thesis
University of Veterinary Medicine Vienna

Submitted by
Hannah Tiefenbrunner

Vienna, July 2022

External supervisor: Ao. Univ. Prof.ⁱⁿ Dr.ⁱⁿ med. Birgit Willinger

External practical supervisor: Kathrin Spettel, MSc

Internal supervisor: Univ.-Profⁱⁿ Dipl.-Ingⁱⁿ Drⁱⁿ rer.nat. Monika Ehling-Schulz

Reviewer: Prof. Dr. Walter Buzina

Acknowledgements

I hereby want to thank Ao. Univ. Prof.ⁱⁿ Dr.ⁱⁿ med. Birgit Willinger for making this master thesis possible and for providing a project on such an interesting and often overlooked subject. I also want to thank her for taking me in even though the microbiology laboratory was a new experience for me and for being such a kind person and thoughtful supervisor.

I want to sincerely thank Kathrin Spettel, MSc, for a great introduction to the microbiology laboratory, for always being there and for “showing me the way”. I further want to thank Kathrin Spettel, MSc and Richard Kriz, BSc for helping me tremendously with the bioinformatic analysis.

I also want to thank Brigitte Selitsch, BA, for helping me out in various matters concerning dermatophytes and for supporting me.

A great thanks goes to Dr. Reinhard Möller, who kindly provided the PathoNostics DermaGenius[®] Resistance and DermaGenius[®] 3.0 Multiplex real-time PCR kits as well as quick technical support.

I am also very grateful to Prof. Dr. med. Pietro Nenoff and Silke Uhrlaß, who kindly provided five terbinafine- and azole resistant dermatophyte strains.

Finally, I want to thank Univ.-Profⁱⁿ Dipl.-Ingⁱⁿ Drⁱⁿ rer.nat. Monika Ehling-Schulz for making this master thesis possible by supporting me as an internal supervisor of the University of Veterinary Medicine as well as the quick feedback.

Table of Contents

1	Introduction	6
1.1	Aim of the Thesis, Research Questions	7
1.2	Establishment of Infection	8
1.3	Terbinafine	9
1.4	Azoles	9
1.5	Resistance Mechanisms in Dermatophytes.....	10
1.5.1	Target Mutation	14
1.5.2	Target Overexpression, Amplification	15
1.5.3	Multidrug Efflux Transporters	16
1.5.4	Drug Degradation	17
1.5.5	Biofilms, Conidia	18
1.5.6	Stress Response	21
2	Methods	23
2.1	Samples	23
2.2	Culture Morphology	24
2.3	Microdilutions.....	25
2.4	DNA Extraction	28
2.5	Induction of <i>In Vitro</i> Resistance	30
2.6	DermaGenius® real-time PCR	31
2.7	PCR Design.....	33
2.8	PCR, Library Prep and NGS.....	34
3	Results	39
3.1	Culture Morphology	39
3.2	Microdilutions.....	42

3.3	Induction of <i>In Vitro</i> Resistance	45
3.4	DermaGenius® real-time PCR	46
3.5	PCR Design.....	48
3.6	PCR, Library Prep and NGS.....	49
4	Discussion.....	55
4.1	<i>Trichophyton indotineae</i> and terbinafine resistance in Austria	55
4.2	Target Mutations in Terbinafine Resistance	58
4.3	Target Mutations in Azole Resistance	59
4.4	PathoNostics DermaGenius® Resistance/3.0 Multiplex real-time PCR	59
4.5	Conclusion and Outlook	61
	Abstract.....	64
	Zusammenfassung	66
	List of Abbreviations	68
	List of Figures.....	69
	List of Tables.....	71
	References	72

1 Introduction

Dermatophytosis (also referred to as tinea or ringworm) is a superficial mycosis of the stratum corneum of the skin, the hair, and the nails of humans and animals caused by dermatophytes. Dermatophytes are primary pathogenic, filamentous fungi that obtain nutrients by the degradation of keratinous material. They thrive at temperatures of 25-28°C and humid conditions, making the skin surface their ideal habitat. Furthermore, dermatophytes are the most common etiological agent causing superficial mycoses, which affect 20-25% of the world population (although incidence varies greatly based on the region). (Havlickova et al. 2008, Baldo et al. 2012)

Dermatophytosis can manifest in a variety of body sites including the trunk (tinea corporis), the legs and groin (tinea cruris), the feet (tinea pedis), the head (tinea capitis), the face (tinea faciei), and the nails (tinea unguium/onychomycosis), leading to scaly plaques which are mildly to severely inflamed. However, over the past few years, a once easily treatable infection has become an epidemic of chronic and recurring dermatophytoses which may take months or even years to subside. As treatment resistance and inflammation of new forms of dermatophytosis increases, patients discomfort increases drastically, calling for an intervention from the medical community. (Havlickova et al. 2008, Verma et al. 2021c)

Dermatophytes exist in the geophilic, zoophilic and anthropophilic domains and consist of the four anamorphic genera *Trichophyton* (*T.*), *Microsporum* (*M.*), *Nannizzia* (*N.*), and *Epidermophyton* (*E.*), which are classified by the morphology of their structures of asexual reproduction termed conidia. (Guarro et al. 1999, Baldo et al. 2012, de Hoog et al. 2017, Martinez-Rossi et al. 2018) Species of all three domains can cause tinea in humans. While zoophilic species cause an acute and strong inflammation caused by a lack of adaptation to the human host, anthropophilic species cause a chronic and persistent infection due to the presence of an adaptive immune response. (Guarro et al. 1999, de Aguiar Peres et al. 2010) The dermatophytes most commonly found in humans are *T. rubrum*, *T. interdigitale* and *T. mentagrophytes*. (Rudramurthy et al. 2018, Salehi et al. 2018, Singh et al. 2018, Khurana et al. 2019, Monod and Méhul 2019, Ebert et al. 2020)

1.1 Aim of the Thesis, Research Questions

The aim of this master thesis is to assess the terbinafine- and azole susceptibility of dermatophyte strains of the *Trichophyton mentagrophytes/interdigitale* species complex in Austria (see Figure 1). Antifungal susceptibility testing of the antifungals amorolfine (AMR), itraconazole (ITC), miconazole (MCZ), terbinafine (TRB), griseofulvin (GRS), ciclopirox (CPX), fluconazole (FLC), and naftifine (NAF) will be performed using the European Committee on Antimicrobial Susceptibility Testing (EUCAST) microdilution method, assessing the minimum inhibitory concentration (MIC) distribution of these antifungals. Terbinafine resistant as well as -susceptible strains will be analysed for *ERG1* target mutations causing resistance using the DermaGenius[®] Resistance Multiplex real-time PCR kit (Cat. No. PN-303, PathoNostics, Maastricht, Netherlands) and Targeted Resequencing by Next Generation Sequencing (NGS). This dual screening allows for the assessment of the DermaGenius[®] Resistance kit, and whether it might be a suitable means of detecting terbinafine resistance in routine screenings.

Furthermore, the possibility of an induction of antifungal *in vitro* resistance (previously reported in *Candida* (Barker et al. 2004)) and *Aspergillus* (Marques De Araujo et al. 2019)) by prolonged exposure to a subinhibitory drug concentrations will be tested. If the induction is successful, the resulting resistant strains will be screened for target mutations to assess the role of target mutations in resistance development in dermatophytes.

Therefore, the main research questions of this thesis are:

- 1) Are there any terbinafine resistant patient isolates of the *T. mentagrophytes/interdigitale* species complex in Austria? Do they belong to the newly discovered species *T. indotineae* (ITS genotype VIII)?
- 2) What is the prevalence of target mutations in *T. mentagrophytes/interdigitale* in Austria?
- 3) Are there any new findings concerning resistance mechanisms in *T. mentagrophytes/interdigitale* in Austria?
- 4) Are there any dominant genotypes in *T. mentagrophytes/interdigitale* in Austrian clinical isolates?

- 5) Are terbinafine and the tested azoles still a good option to treat dermatophytosis caused by *T. mentagrophytes/interdigitale*?

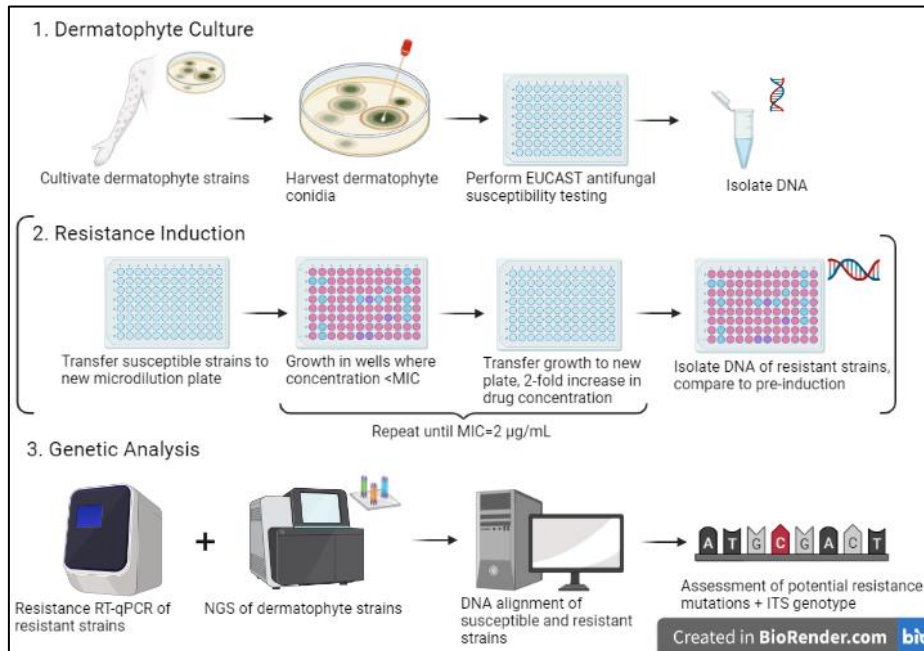


Figure 1: Aims of this master thesis (created with BioRender.com)

1.2 Establishment of Infection

The human body possesses several defences against microbial infections, which include the presence of an intact skin barrier, continuous shedding of the outermost skin layers, fungistatic fatty acids (e.g. undecanoic acid), and the slightly acidic pH of the skin. However, if the skin is damaged or macerated, dermatophytes can invade keratinised structures. Arthroconidia stuck to the skin, hair or nail germinate, and hyphae penetrate the outermost layers while sulphite transporters sequester sulphite into the tissue, digesting keratin into cysteine and S-sulphocysteine, then into peptides and amino acids. Therefore, the secretion of sulphite as well as enzymes such as nucleases, lipases, and other nonspecific proteases provides nutrients and thereby allows for the survival and establishment of the dermatophyte. (Maranhão et al. 2007, Martinez-Rossi et al. 2008) Once the dermatophyte is established in the host tissue, fungal mannans and the iC3b receptor act in an immunosuppressive manner against phagocytes, enabling the fungus to persist. Vegetative conidia and biofilms (such as in dermatophytoma) contribute to the persistence of infection despite the host immune system and some therapeutic interventions. (Martinez-Rossi et al. 2008, Baldo et al. 2012)

1.3 Terbinafine

Terbinafine (TRB) has been the gold standard of care for dermatophytosis for several years. Originally isolated from *Streptomyces* sp. KH-F12, this orally and topically administered drug belongs to the class of allylamine antifungals. (Campoy and Adrio 2017) The popularity of terbinafine is largely due to its favourable pharmacokinetics, relatively low toxicity, lack of drug interactions, and consistent drug levels in the stratum corneum due to high keratin adherence. (Faergemann et al. 1994, Salehi et al. 2018, Khurana et al. 2019, Verma et al. 2021a)

Allylamines (terbinafine, naftifine, butenafine) act in a fungistatic- as well as in fungicidal manner by inhibiting ergosterol biosynthesis via the inhibition of squalene epoxidase (SQLE, SE, encoded by the *ERG1* gene), which drives the conversion of squalene to 2,3-oxidosqualene. Ergosterol is the main sterol in fungal cell walls, functioning as a key element in cell wall integrity and -fluidity as well as in the regulation of membrane-bound enzymes. Ergosterol inhibition through the inhibition of squalene epoxidase leads to the depletion of ergosterol as well as to the accumulation of squalene, which is a toxic, membrane-disrupting intermediate (fungicidal mechanism of action). Furthermore, ergosterol has an additional “sparkling” function that enables fungal cells to start into the cell cycle and to proliferate. Therefore, the complete depletion of ergosterol in the fungal cell leads to a halt of cell cycle progression (fungistatic mechanism of action). (Martinez-Rossi et al. 2008, Khurana et al. 2019)

1.4 Azoles

Azoles are the largest class of antifungals currently used against dermatophytes and feature the possibility of local- as well as systemic application. The azoles are divided into imidazoles (first generation azoles), and triazoles (second/third generation azoles). The group of imidazoles contains ketoconazole, clotrimazole, miconazole, luliconazole, econazole, bifonazole, sertaconazole, and tioconazole. Imidazoles are mainly administered topically due to poor oral bioavailability and toxicity. Triazoles feature better bioavailability, pharmacokinetics and pharmacodynamics, as well as a broader activity spectrum. They consist of fluconazole, itraconazole, voriconazole, posaconazole, isavuconazole, ravuconazole, and laniconazole. (Ghannoum 2016)

Similar to allylamines, azoles also inhibit ergosterol biosynthesis. However, azoles act on the cytochrome P-450-dependent enzyme lanosterol 14 α demethylase (encoded by *ERG11*) by

binding an iron atom in its active site, thereby blocking the enzyme. The exact mechanism of action varies slightly between imidazoles and triazoles. Imidazoles alter the activity of membrane-bound enzymes, and some bind to lipids directly. As a result, 14 α -methylated sterols accumulate and are converted to fungistatic metabolites (-dienol). Triazoles, on the other hand, exclusively inhibit lanosterol 14 α demethylase. The rising azole resistance are suspected to be due to the fungistatic rather than fungicidal nature of azoles. (Cauwenbergh et al. 1988, Sanati et al. 1997, Hazen 1998, White et al. 1998, Paião et al. 2007, Campoy and Adrio 2017, Shukla et al. 2018, Song et al. 2018, Khurana et al. 2019)

The most-commonly prescribed azole is itraconazole, though a wide variety of azoles is used against dermatophytes (especially in India). In some case, miconazole, luliconazole, and lanoconazole are prescribed, while more unknown azoles such as econazole are rarely used. Fluconazole was a commonly used azole several years ago, but due to increasing resistance rates, it is not prescribed as often nowadays. Voriconazole, posaconazole and isavuconazole have been reported as a last resort in treatment-resistant cases. (White et al. 1998, Vandeputte et al. 2012, Khurana et al. 2019, Shaw et al. 2020, Verma et al. 2021a)

1.5 Resistance Mechanisms in Dermatophytes

When terbinafine first came into use in the 1990s, no cases of terbinafine-resistant strains were known. The first cases of *in vitro* resistance were reported in the early 2000s (Hofbauer et al. 2002, Osborne et al. 2003, Khurana et al. 2019), and the first reports of treatment resistance were published in 2003 (Mukherjee et al. 2003) and 2006 (Osborne et al. 2006).

Since then, the number of treatment-resistant strains has grown exponentially, and India has been in the centre of this resistance development. (Singh et al. 2018, Shankarnarayan et al. 2020, Shaw et al. 2020, Gaurav et al. 2021) This localized increase of resistance rates has mainly been attributed to the over-the counter availability of creams containing potent corticosteroids in combination with antifungals, leading to erratic self-medication by patients. These combination creams are known for hindering the clearance of the infection through suppression of the immune system as well as featuring a plethora of side effects. The erratic use of these creams also leads to subinhibitory drug concentrations, promoting the development of antifungal resistance. However, improper treatment regimens and nonadherence to

prescribed treatment regimens have also been identified as factors contributing to resistance development. Furthermore, factors such as the socioeconomic status of patients, environmental circumstances, increasing population density and travelling contribute to the increased spread of resistant strains. (Nenoff et al. 2020, Gaurav et al. 2021, Verma et al. 2021b, 2021c) However, research interest in this field has only been piqued within the past years, as a report from (Panda and Verma 2017) shows.

Not only the antifungal susceptibility patterns, but also the species distribution of dermatophytes isolated from patients has changed. Until around 2012, the majority of clinical isolates were categorized as *Trichophyton rubrum*, an anthropophilic dermatophyte. This species has almost exclusively been replaced by *Trichophyton mentagrophytes*, an originally zoophilic strain which has adapted to the human host by a process termed “anthropisation”. (Nenoff et al. 2019b)

As the clinical prevalence of certain dermatophyte species has changed and as novel (in some cases highly resistant) strains have appeared, the classification of dermatophytes has become a key factor of recent studies. Currently, ten variants of *T. mentagrophytes* and *T. interdigitale* have been verified based on the genotype of the internal transcribed spacer (ITS) region. These ITS genotypes are further distinguished by the geographic location from which they originate (see Table 1). (Verma et al. 2021b)

Table 1: ITS genotypes and geographic origins of the *T. mentagrophytes/interdigitale* complex; data taken from (Verma et al. 2021b)

ITS genotype	Origin
Type I	Europe
Type II	Cosmopolite
Type III	Europe
Type III*	Cosmopolite
Type IV	UK, USA, South Africa, France
Type V	Asia, Egypt, Iran, Iraq, Japan
Type VI	Europe, Russia, Finland
Type VII	Thailand
Type VIII	Asia, India, Iran, Oman, Australia
Type IX*	Australia

The ITS variant most prevalent in resistance development is *T. mentagrophytes* Type VIII, which was first described in India (also called *Trichophyton indotineae* (Kano et al. 2020)), and which has reportedly caused an epidemic-like scenario of (in some cases multi-) resistant dermatophytosis in India. The rise of this multi-resistant genotype is likely due to the pervasive use of over the counter fixed-dose combination creams containing potent corticosteroids (clobetasol propionate, betamethasone dipropionate, beclomethasone dipropionate) and antifungals. The resulting steroid-modified tinea manifests as eczematous, annular lesions without central clearing that spread concentrically. The appearance of several borders is common after sporadic corticosteroid use. (Nenoff et al. 2019b, Singh et al. 2019, Shaw et al. 2020, Verma et al. 2021a, 2021b, 2021c)

Cases of the Indian genotype VIII have been reported in Germany (Burmester et al. 2019, Süß et al. 2019, Nenoff et al. 2020), Switzerland (Klinger et al. 2021), Greece (Siopi et al. 2021), Estonia (Saunte et al. 2021), Iceland (Saunte et al. 2021), Finland (Järv et al. 2019), France (Dellièvre et al. 2022), Slovenia (Saunte et al. 2021), Sweden (Saunte et al. 2021), Japan (Kano et al. 2020, Noguchi et al. 2021), and Iran (Taghipour et al. 2020). (Brasch et al. 2021) recently reported the occurrence of *T. indotineae* in Germany as early as 2011.

Furthermore, (Pashootan et al. 2022) recently published a report featuring *T. mentagrophytes* strains with the novel ITS genotype XXIX, which seems to be more closely related to ITS genotype II* than genotype VIII. The authors reported this genotype as having a higher MIC₅₀ values than *T. indotineae*.

Overall, antifungal susceptibility rates are increasing world-wide. Terbinafine MIC values are reaching unprecedented heights of ≥ 32 $\mu\text{g/mL}$ in a variety of treatment center-specific as well as nation-wide studies. (Khurana et al. 2018, Rudramurthy et al. 2018, Singh et al. 2018, Shaw et al. 2020) However, currently only few epidemiological cut-off (ECOFF) values and no clinical breakpoints have been established for dermatophytes, which complicates the identification of resistant strains in diagnostic centres. However, some studies (Yamada et al. 2017, Nenoff et al. 2020) have established a terbinafine breakpoint of ≥ 0.2 $\mu\text{g/mL}$ and a wild-type cut-off of ≤ 0.25 $\mu\text{g/mL}$ for azoles.

Cases of terbinafine-resistant isolates have been reported in Switzerland (Yamada et al. 2017, Hsieh et al. 2019), Denmark (Saunte et al. 2019, Astvad et al. 2022), Belgium (Sacheli et al. 2020), Poland (Gnat et al. 2020), Japan (Kakurai et al. 2020, Kimura et al. 2020), and Malaysia (Nizam et al. 2016).

Elevated MIC values were also reported for fluconazole (≥ 32 $\mu\text{g/mL}$) (Manzano-Gayosso et al. 2007, Mota et al. 2009, Khurana et al. 2018, Pathania et al. 2018, Rezaei-Matehkolaei et al. 2018, Rudramurthy et al. 2018, Singh et al. 2018, Shaw et al. 2020, Jiang et al. 2021), itraconazole and/or ketoconazole (Gupta and Kohli 2003, Manzano-Gayosso et al. 2007, Mota et al. 2009, Khurana et al. 2018, Salehi et al. 2018, Singh et al. 2018), miconazole and/or sertaconazole (Khurana et al. 2018, Singh et al. 2018), clotrimazole (Singh et al. 2018), and voriconazole (Salehi et al. 2018, Singh et al. 2018).

(Saunte et al. 2021) recently published an alarming report describing terbinafine and azole resistance in Bosnia & Herzegovina, Switzerland, Denmark, Estonia, Finland, Greece, Iceland, Italy, Lithuania, Malta, Norway, Russia, Serbia, Slovenia, Spain, Sweden, and the United Kingdom. While some of these strains were identified as *Trichophyton mentagrophytes* genotype VIII, others were classified as *Trichophyton*, *Microsporum* or *Nannizzia*, highlighting that antifungal resistance is not just present in one single species or ITS genotype. Of all

assessed isolates, Saunte et al. reported 64% to be resistant to terbinafine, 41% to itraconazole, in 16% to fluconazole, and 4% to griseofulvin.

(Singh et al. 2019) also reports the rise of a novel *Trichophyton* population resistant to terbinafine (MIC 4 - ≥ 32 $\mu\text{g/mL}$), as well as fluconazole (MIC 32 - ≥ 64 $\mu\text{g/mL}$) and griseofulvin (geometric mean MIC ≥ 4 $\mu\text{g/mL}$). (Singh et al. 2018) also reports a prevalence of 55% for simultaneous TRB/sertaconazole/FLC resistance and of 20% for simultaneous TRB/ITC/sertaconazole/FLC resistance in *T. interdigitale* clinical isolates in Delhi. The combination of terbinafine and azole resistance is especially worrying since azoles (especially itraconazole) are the main treatment option in terbinafine resistant strains. (Shaw et al. 2020, Gupta et al. 2021, Verma et al. 2021a) For further understanding, (Shaw et al. 2020) provides a highly comprehensive review on the distribution of azole and terbinafine MIC values in dermatophytes.

1.5.1 Target Mutation

Target mutations are the most prominent resistance mechanism in dermatophytes. These coding mutations lead to a change in amino acid sequence through the insertion, deletion, or substitution of nucleotides in the gene of the protein targeted by the antifungal. The changes in amino acid sequence then lead to impaired drug-target binding, ultimately resulting in antifungal resistance. Usually, target mutations confer cross-resistance to all drugs of the same class, as drugs of one antifungal class target the same enzyme. (Tsai et al. 2004, Osborne et al. 2005, 2006, Pasrija et al. 2005, Martinez-Rossi et al. 2018, Zhang et al. 2019, Kong et al. 2021)

Target mutations leading to terbinafine resistance were first reported in 2005 by (Osborne et al. 2005). The target of terbinafine is the enzyme squalene epoxidase (encoded by the *ERG1/SQLE* gene), a crucial part of the ergosterol synthesis pathway (see 1.3). The most common *ERG1* target mutations lead to the amino substitutions p.F397L and p.L393F, which account for a vast majority of resistant isolates. However, various other substitutions (p.I121M + p.V237I, p.L335F + p.A448T, p.L393S, p.S395P + p.A448T, p.F397L + p.Y394N, p.F397 + p.A448T, p.F397I, p.F397V, p.Q408L, p.F415I, p.F415S, p.F415V, p.H440Y, p.H440Y + p.F484Y, p.S443P) have been found. (Osborne et al. 2005, 2006, Yamada et al. 2017, Singh et al. 2018, Hsieh et al. 2019, Saunte et al. 2019, Ebert et al. 2020, Shankarnarayan et al. 2020)

The impact of amino acid substitutions on the drug-target binding of terbinafine to the squalene epoxidase protein of *T. rubrum* was shown by (Saunte et al. 2019) (see Figure 16). This model shows that certain target mutations result in amino acid substitutions in the binding site, thereby impairing drug-target binding.

The drug target of azoles is lanosterol 14 α demethylase, which is encoded by the *ERG11/CYP51* gene. ((Song et al. 2018), see 1.4) Target mutations have a varying impact on azole-target binding, since the exact binding site varies depends on the distinct azole used. (Martinez-Rossi et al. 2018)

While a variety of *ERG11* mutations leading to azole resistance has been reported in *Candida* (Vandeputte et al. 2012, Martinez-Rossi et al. 2018), no *ERG11* target mutations have been found in dermatophytes so far. However, the *ERG1* mutation A448T recently discovered in *T. indotineae* (*T. mentagrophytes* ITS genotype VIII) has been linked to elevated azole MIC values in combination with average terbinafine MIC values, though the resistance mechanism is yet unknown. (Burmester et al. 2020, Ebert et al. 2020) Furthermore, *ERG1* double mutants carrying the resistance mutations F397L and A448T have been shown to feature increased fluconazole resistance rates in combination with terbinafine resistance. (Burmester et al. 2020)

1.5.2 Target Overexpression, Amplification

Azole resistance induced by the overexpression of the *ERG11* gene, which leads to an increased production of the target enzyme has been reported in *Candida*, but not yet in dermatophytes. The overexpression of *ERG11* by gene duplication in *Candida* is either due to the formation of an isochromosome, which contains two copies of the left arm of chromosome 5 harbouring the *ERG11* gene, or due to the duplication of the entire chromosome. However, *ERG11* overexpression in *Candida* can also be the result of activating mutations in the transcription factor *Upc2*. (Selmecki et al. 2006, Dunkel et al. 2008, Cowen et al. 2015, Sanglard 2016, Campoy and Adrio 2017)

Even though these resistance mechanisms have not yet been found in dermatophytes, (Diao et al. 2009) found a 13.55-fold upregulation of 14- α sterol demethylase in *T. rubrum* in response to exposure to sub-inhibitory concentrations of itraconazole. As a result, it might be possible that further studies will reveal similar resistance mechanisms in dermatophytes.

1.5.3 Multidrug Efflux Transporters

Efflux pumps (multidrug efflux transporters) are a group of membrane-bound proteins that extrude a variety of chemically and structurally dissimilar, hydrophobic compounds which could potentially harm the cell. The overexpression of multidrug efflux transporters leads to an increased efflux of toxic compounds, thereby leading to antifungal resistance. Due to the broad range of potential substrates, the overexpression of efflux pumps usually causes resistance to several drug classes (multidrug resistance). (Neyfakh 2002, Martinez-Rossi et al. 2018, Pai et al. 2018, Khurana et al. 2019)

The most prevalent multidrug efflux transporter superfamily is the ATP Binding Cassette (ABC) transporter superfamily, which consists of primary membrane transporters that hydrolyse ATP in order to extrude their substrate. The ABC transporter superfamily consists of five families, of which three are extensively studied: The multidrug resistance (MDR), the MDR-associated protein (MRP) and the pleiotropic drug resistance (PDR) family. (Pai et al. 2018, Khurana et al. 2019)

(Fachin et al. 2006) first described the role of the *TruMDR2* gene isolated from *T. rubrum*. While the authors could not find an upregulation of *TruMDR2* after 15 minutes of terbinafine exposure, they reported an upregulation in response to fluconazole, ketoconazole, and tioconazole, and a strong upregulation in response to itraconazole. Similarly, (Paião et al. 2007) found that *TruMDR2* was upregulated 6.4-fold after terbinafine exposure and 13.1-fold after fluconazole exposure.

In 2006, (Cervelatti et al. 2006) reported the upregulation of the related transporter gene *TruMDR1* in *T. rubrum* after 30 minutes of ketoconazole, fluconazole (highest upregulation), and itraconazole exposure, but not after exposure to terbinafine or tioconazole.

(Monod et al. 2019) aimed to find the cause of azole resistance in dermatophytes by transforming a library of plasmids of an azole-resistant *T. rubrum* strain into *Saccharomyces (S.) cerevisiae*. The plasmid DNA of resistant clones was then transformed into *Escherichia coli*, which became resistant to ampicillin. From these resistant clones, a novel gene was isolated and named *TruMFS1*. The authors also transformed *TruMFS2* into *S. cerevisiae*, which led to voriconazole and fluconazole resistance.

Furthermore, the authors investigated the role of *TruMDR1*, *TruMDR2*, *TruMDR3* and *TruMDR5* in azole resistance. The expression of *TruMDR1* led to voriconazole, fluconazole, and miconazole resistance in *S. cerevisiae*, while the expression of *TruMDR2* or *TruMDR5* led to itraconazole resistance. Only the expression of *TruMDR3* rendered the yeast resistant to all azoles. The azole-resistant strain TIMM20092 was shown to overexpress *TruMDR2* and *TruMDR3* 5 to 8-fold, and *TruMDR1*, *TruMDR4*, *TruMDR5*, *TruMFS1*, and *TruMFS2* 2 to 4-fold. Exposure to itraconazole and voriconazole significantly increased the expression of *TruMDR3*, and exposure to itraconazole slightly increased the expression of *TruMDR1* and *TruMDR2*. Similarly, the deletion of *TruMDR3* led to voriconazole susceptibility and slightly decreased itraconazole susceptibility. Therefore, this article supports the previous hypothesis *TruMDR1* and *TruMDR2* are involved in azole resistance, and sheds light on a newly found MDR gene.

(Kano et al. 2018) reported a 2 to 4-fold upregulation of the transporters *MDR1*, *MDR2*, *MDR4*, and *PDR1* in a terbinafine treatment-resistant strain of *M. canis* in response to TRB exposure. The MIC of the treatment-resistant strain was determined as $> 32 \mu\text{g/mL}$ but was reduced to $8 \mu\text{g/mL}$ upon addition of the efflux blocker FK506, which strengthens the hypothesis that multidrug efflux transporters are involved in terbinafine resistance, although another mechanism might have also been at play.

Finally, (Martins et al. 2016) reported a significant upregulation of *PDR1* in *T. tonsurans* and *T. equinum*, of *MDR2* in *T. rubrum* and *T. equinum*, and of *MDR4* in *T. equinum* and *T. interdigitale* in response to terbinafine exposure. The authors also reported that *MDR4* compensates for a lack of *MDR2* in ΔMDR2 knockout mutants challenged with griseofulvin, which supports the hypothesis that multidrug efflux transporters might compensate for each other.

1.5.4 Drug Degradation

While antimicrobial resistance by drug degradation is usually a feature found in bacteria, this phenomenon was described in *Aspergillus nidulans*. Graminha et al. created plasmids conferring terbinafine resistance from a naturally resistant *Aspergillus nidulans* strain. After sib selection, the terbinafine resistance was determined to be due to the expression of salicylate 1-

monooxygenase (*sala* gene). Salicylate 1-monooxygenase, an enzyme involved in the naphthalene metabolism in bacteria such as *Pseudomonas putida*, is able to degrade terbinafine as terbinafine contains a naphthalene nucleus. Additionally, the authors discovered that while in a naturally resistant strain, *sala* expression is dependent on and proportional to terbinafine exposure, the transformed strain constitutively expressed *sala*. (Graminha et al. 2004)

These findings were supplemented by (Santos et al. 2018) who cloned the *sala* gene of wildtype *T. rubrum* and transformed it into a wild-type isolate of the same strain, which resulted in slightly elevated terbinafine MIC values (0.0976 µg/mL instead of 0.0244 µg/mL). The authors reported that *sala* gene expression was upregulated after TRB exposure in a quantity-specific manner (multicopy effect), and that resistance by *sala* was lost after six serial passages in absence of terbinafine exposure. However, further studies will need to be performed on this resistance.

So far, no natural azole resistance due to drug degradation has been reported in dermatophytes.

1.5.5 Biofilms, Conidia

Biofilms are sessile microbial colonies embedded into an extracellular matrix composed of polysaccharides, proteins, and nucleic acids. Furthermore, biofilms are often categorized by the presence of so-called persister cells, which are more tolerant towards antimicrobial therapy. This increased tolerance to external stressors is likely due to several factors: The physical barrier created by the biofilm, reduced contact to the host's immune system, increased expression of efflux pumps of cells in a biofilm (see section 1.5.3), and secreted proteins. (Costa-Orlandi et al. 2014, Borghi et al. 2016, Brilhante et al. 2019)

While biofilms have been described abundantly in *Candida*, dermatophyte biofilms have been investigated relatively sparsely. (Costa-Orlandi et al. 2014) However, (Costa-Orlandi et al. 2014) reported that *Trichophyton rubrum* and *Trichophyton mentagrophytes* form biofilms on coverslips *in vitro* and first described dermatophyte biofilm morphology as well as metabolic activity.

(Brilhante et al. 2018) also tested the antifungal susceptibility of planktonic cells and biofilms to voriconazole (VCZ), itraconazole and griseofulvin. While planktonic MIC values were low, a drug concentration of 50-fold the MIC was necessary to significantly reduce metabolic

activity of cells inside a biofilm, highlighting the protective environment generated by a biofilm. (Brilhante et al. 2019) further established a model for the cultivation of dermatophyte biofilms on cat and dog hair *ex vivo*.

These studies were complemented by (Castelo-Branco et al. 2020) who generated biofilms of *Microsporum canis* and *Trichophyton mentagrophytes in vitro*, consequently performing antifungal susceptibility testing of planktonic cultures as well as biofilms. Planktonic cultures featured MIC ranges of 0.125-1 µg/mL for griseofulvin, and 0.00097-0.25 µg/mL for itraconazole and terbinafine. In contrast, MIC ranges obtained for sessile cultures were 2- >512 µg/mL for griseofulvin, and 0.25- >64 µg/mL for itraconazole and terbinafine. However, all tested antifungals significantly reduced the metabolic activity and biomass of the biofilm compared to the drug-free control. Moreover, a slight reduction of fungal structures as well as a disorganized structure of the extracellular matrix could be found in response to antifungal treatment *ex vivo* (biofilms on cat hair).

One of the main causes of treatment failure in onychomycosis is the formation of dermatophyte biofilms (dermatophytoma) under the nail plate. While dermatophytes inside a biofilm are generally exposed to lower antifungal concentrations, drug penetration is reduced even more in sites such as the nail. Furthermore, dermatophytoma contain vast amounts of spores (in clinical settings mostly asexual conidia), which are vegetative structures of reproduction that can endure harsh conditions not suitable for living organisms. Dermatophyte conidia are either generated via lateral or terminal budding of hyphae (simply referred to as conidia), or via the fracture of hyphae at septum level (referred to as arthroconidia). Usually, conidia are produced *in vitro* on Sabouraud medium, while arthroconidia are produced *in vivo* inside the host. Most importantly, conidia significantly complicate antifungal treatment due to their high antifungal tolerance. As a result, several research teams have started assessing the antifungal susceptibility of living dermatophytes and conidia inside a nail to combat treatment resistance and relapse in onychomycosis. (Burkhart et al. 2002, Faway et al. 2018, Martinez-Rossi et al. 2018, Khurana et al. 2019)

(Yazdanparast and Barton 2006, Tabart et al. 2007, 2008) were able to produce arthroconidia under increased CO₂ pressure (10%), at pH 7.5 and 37°C. Furthermore, the authors found that

subinhibitory concentrations of amphotericin B, griseofulvin and clotrimazole increased arthroconidia production, while itraconazole and terbinafine suppressed it.

(Osborne et al. 2004) further reported that the terbinafine minimum fungicidal concentration (MFC) of *T. rubrum* in culture with nail powder is much higher than when using the Clinical & Laboratory Standards Institute (CLSI) microdilution procedure (CLSI M38-A: MFC=0.016-0.030 µg/mL, nail culture: MFC=1.0-2.0 µg/mL). Further, the treatment duration in nail culture was prolonged to 4 weeks.

(Seebacher 2003) reported a terbinafine MIC of 0.02 µg/mL for proliferating dermatophytes, but of 2.0 µg/mL for dormant stages (referred to as both arthrospores and arthroconidia). The author found that after patient medication with 250 mg terbinafine daily for one week, terbinafine concentrations in the tissue were as follows: Plasma 1.01 µg/mL, sebum 5.18 µg/g, stratum corneum 1.63 µg/g, hair 1.05 µg/g, and nail 0.52 µg/g. These values indicate that the terbinafine concentration in the nail post-treatment is well below the MIC value of dermatophyte arthrospores [sic], which might lead to the survival of arthrospores [sic] inside the nail. As a result, “live” arthrospores [sic], which cannot be detected using routine tests will remain inside the nail and cause relapse.

Similarly, (Arrese et al. 2001) emphasized that *in vitro* resistance testing does not compare to onychomycosis, since onychomycosis is largely influenced by the presence of arthroconidia. As a countermeasure, the authors stress the use of the corneofungimetry bioassay, which uses human stratum corneum to test the antifungal susceptibility of a strain of interest *ex vivo*. Furthermore, the authors suggest the use of “boosted oral antifungal therapy” (BOAT) and “boosted antifungal topical therapy” (BATT), which consists of applying a piece of agar to the affected nail. Thereby, these methods are supposed to induce the germination of arthroconidia and result in increased treatment success.

However, conidia might not be the only factor at play in antifungal resistance in onychomycosis. Certain genes involved in antifungal resistance and -response such as *TruMDR2* (Fachin et al. 2006, Maranhão et al. 2009, Petrucelli et al. 2019), *hsp70* (Martinez-Rossi et al. 2016), *hsp90* (Jacob et al. 2015), and *pacC* (Ferreira-Nozawa et al. 2006) were shown to be upregulated during dermatophyte growth on nails. Furthermore, (Gupta et al. 2021)

noted that mixed infections with non-dermatophyte moulds contribute to the recent rise of treatment-resistant onychomycosis cases.

1.5.6 Stress Response

Fungi adapt to a variety of environmental conditions and stressors such as changes in temperature, pH or antifungal therapy by altering their metabolism. While stress responses aren't considered an antifungal resistance mechanism per se, these changes can stabilize the fungal cell during treatment, enabling other resistance mechanisms to take effect. (Martinez-Rossi et al. 2016, Pai et al. 2018) However, as the fungal gene expression not only adapts to antifungals, but to a variety of environmental factors, connections between stress response and antifungal resistance should be considered carefully.

(Paião et al. 2007) first discovered the upregulation of several novel proteins possibly related to cellular stress response in response to terbinafine and fluconazole exposure in *T. rubrum*. These included proteins similar to MDR-like proteins of *Aspergillus* species (fluconazole exposure), a copper resistance-associated P-type ATPase protein likely involved in copper homeostasis (terbinafine and fluconazole exposure), a never in mitosis A (NIMA) interactive protein, a DNA mismatch repair protein, a carboxylic ester hydrolase and a Pol protein. The authors note that the Pol protein shows similarities to the *C_{gret}* retrotransposon from *Glomerella cingulata*, which might suggest the involvement of transposable elements in *T. rubrum* stress response.

(Petrucci et al. 2019) performed a large-scale transcriptome analysis of *T. rubrum* cultured in the presence of keratinocytes in response to terbinafine exposure and found 277 differentially expressed genes. The upregulated genes included ABC and major facilitator superfamily (MFS) transporters, the transcription factor C2H2, a glycosyl hydrolase and N-acetylglucosamine (GlcNAc). Repressed genes included genes of the ergosterol synthesis pathway (*ERG1*, *ERG2*, *ERG4*, *ERG5*, *ERG11* and *ERG25*), the sulfite efflux pump *SSU1*, β -lactamases, metallo- β -lactamases and thioredoxin. Most repressed genes were involved in ribosomal pathways or in the ribonucleoprotein complex, while induced genes were membrane proteins, involved in transmembrane transport or in ATP binding. (Zhang et al. 2009) reported similar results: *ERG2*,

ERG4, *ERG24*, and *ERG25* were downregulated, while *ERG10*, *ERG13* and *INO1* were induced.

(Peres et al. 2010) reported similar results to Paião and Petrucelli in *T. rubrum* in response to terbinafine, fluconazole, itraconazole, ketoconazole and tioconazole exposure. Additionally, the authors reported an upregulation of the *sala* gene in response to terbinafine and fluconazole exposure (see 1.5.4).

(Yu et al. 2007) reported an upregulation of the *ERG3*, *ERG4*, *ERG6*, *ERG11*, *ERG24*, *ERG25* and *ERG26* genes involved in ergosterol biosynthesis as well as an upregulation of *CPR* (*P450R*) in *T. rubrum* in response to ketoconazole exposure. *CPR* was previously shown to cause ketoconazole resistance upon disruption (Venkateswarlu et al. 1998).

Similarly, (Diao et al. 2009) reported an upregulation of *ERG7*, *ERG24*, *ERG25*, *ERG26*, *ERG6*, and *ERG11* in response to itraconazole exposure in *T. rubrum*. Since most of these genes (all except *ERG7*) are downstream of *ERG11*, the authors argued that their induction could be a response to the ergosterol depletion induced by azoles. Furthermore, genes involved in the biosynthesis of inositol-containing compounds, cell wall integrity, and homologues of multidrug efflux transporters (*Pdr5*) were induced. Genes of the amino acid metabolism, energy production and conversion, coenzyme transport and metabolism, protein biosynthesis, carbohydrate metabolism, and energy generation and conversion were typically repressed.

(Jacob et al. 2015) reported a significant upregulation of the heat shock protein genes *hsp20*, *hsp60*, *hsp88-like*, and *hsp90* in *T. rubrum* following terbinafine exposure. The chemical inhibition of Hsp90 lead to a 10-fold increase in azole susceptibility as well as decreased growth on human nail *in vitro*.

Similarly, (Martinez-Rossi et al. 2016) reported an induction of *hsp20/hsp30* (unpublished results), *hsp70*, *hsp90* co-chaperone *cdc37*, *hsf1*, *HspSsc1*, and *pacC* in *T. rubrum* in response to terbinafine exposure, while *hsp20/hsp30* were upregulated in response to itraconazole. HSPs are a class of highly conserved proteins that assist in protein folding and refolding, assigning misfolded proteins to be degraded and assuring proteome integrity and homeostasis. HSPs enable the dermatophytes to survive challenging conditions by responding to environmental

stresses such as thermal stress, antifungal drugs, oxidative stress, heavy metal exposure, and others. (Jacob et al. 2015)

Finally, (Bitencourt et al. 2020) recently discovered that Hac1/HacA, which is a crucial part of the unfolded protein responses, plays a major role in *T. rubrum* stress response. Hac1/HacA is activated following cleavage by the transmembrane sensor Ire1/IreA in response to the accumulation of misfolded proteins in the endoplasmic reticulum. While terbinafine and griseofulvin activated HacA, HacA deletion majorly impaired virulence factors such as growth on keratin, hyphal development, thermotolerance, and protoplast regeneration. Furthermore, HacA deletion led to an increased susceptibility to ketoconazole, DTT, and compounds acting on the cell wall as well as reduced growth rates, though terbinafine susceptibility was decreased. Furthermore, the culture pigmentation in keratin culture changed (shift in secondary metabolites), the ergosterol content decreased in knock-outs, and the secretion of keratinolytic proteases was increased. Changes in the mannosyltransferases also lead to an altered immune response in cell culture. (Bitencourt et al. 2020)

As the need for new classes of antifungals rises exponentially due to the rise of antifungal resistance, inhibitors of cellular pathways of the stress response such as Hsp90, calcineurin, and Ras1 amongst others, are being developed. (LeBlanc et al. 2020)

2 Methods

2.1 Samples

Dermatophyte strains were gathered from several Austrian clinics in Vienna, Graz, Linz, Klagenfurt, and Wiener Neustadt. The species distribution of all dermatophyte strains currently part of the dermatophyte culture collection of the Division of Clinical Microbiology of the General Hospital of Vienna (not the sample population used in this study) is depicted in Figure 2. Since the current scenario of terbinafine-resistant dermatophytosis is largely due to strains belonging to the *T. mentagrophytes/interdigitale* species complex, this master thesis will focus on the susceptibility patterns of 106 strains of this complex. Of 106 strains in total, 52 strains

were clinical isolates, 39 strains were laboratory control strains such as from NEQAS/INSTAND, and the 15 strains were of unknown origin.

Additionally, Prof. Dr. med. Pietro Nenoff and Silke Uhrlaß from the Labor Mölbis in Mölbis, Germany kindly provided four strains of *Trichophyton mentagrophytes* with the ITS Genotype VIII (*Trichophyton indotineae*; strain IDs 214677/16, 216377/17, 901538/18, 205667/19) and one *Trichophyton rubrum* strain, which was resistant to terbinafine but did not grow due to unknown reasons. Two *Trichophyton indotineae* strains (214677/16, 216377/17) were terbinafine resistant and itraconazole susceptible, and two strains (901538/18, 205667/19) were terbinafine susceptible and itraconazole resistant. The *Trichophyton indotineae* strains were used as reference strains since their resistance patterns and mutations are known. More information on these strains can be found in (Nenoff et al. 2020).

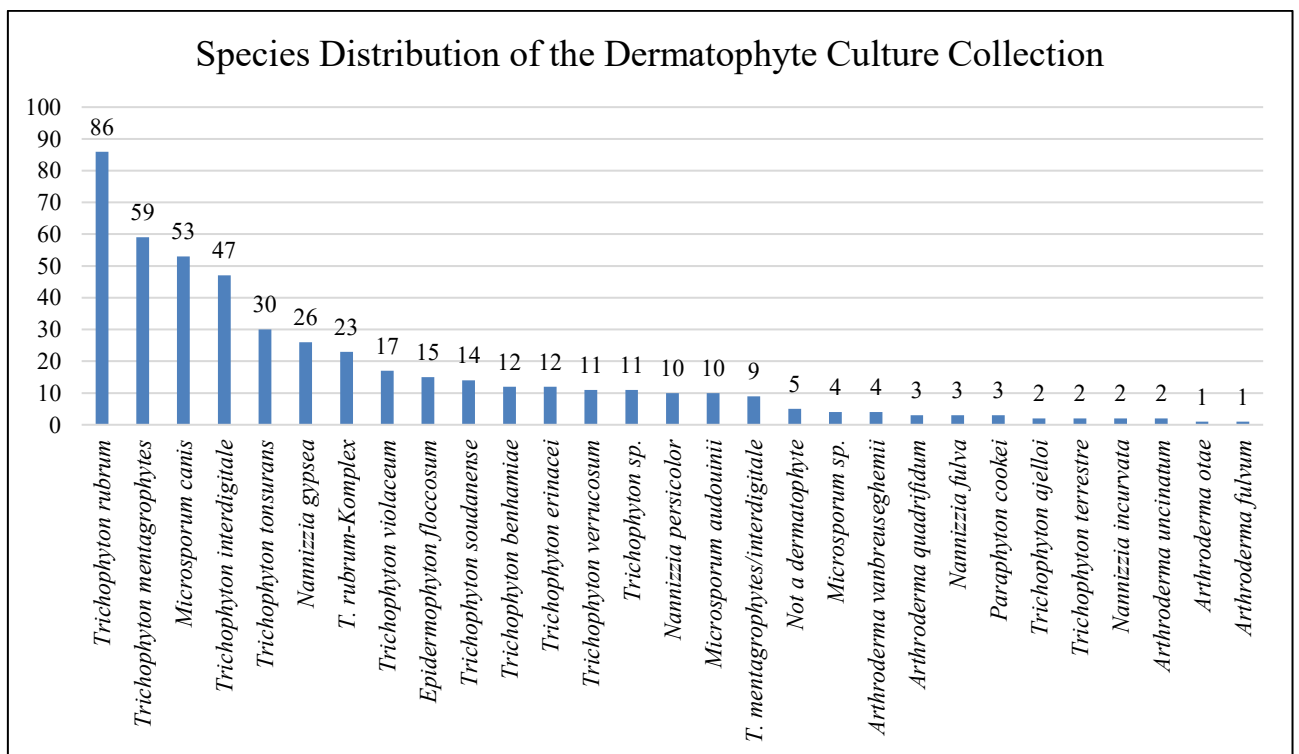


Figure 2: Species distribution of the dermatophyte culture collection of the Department of Clinical Microbiology, General Hospital of Vienna

2.2 Culture Morphology

The macroscopic culture morphology of dermatophyte isolates was assessed by visual inspection of the fungal colonies cultivated on Sabouraud dextrose agar or malt extract agar for

approximately seven days. Microscopic analysis was performed by staining a thin layer of fungal material with lactophenol blue using the tape method and by analysing the slide using brightfield microscopy. More specifically, stained microscope slides were prepared by lightly touching the surface of a fungal culture with the adhesive side of a scotch tape strip. The tape was placed specimen-side down in a drop of lactophenol blue on a microscope slide. Brightfield microscopy was performed at 10x, 40x, and 100x magnification. 100x magnification was performed with the aid of immersion oil.

2.3 Microdilutions

Since the development of antifungal resistance in dermatophyte strains is a relative new development, no clinical breakpoints and only few epidemiological cut-offs (ECOFFs) have been set so far. Therefore, the total distribution of MIC values found in our study as well as the following MIC values were used to categorize the MIC levels of the dermatophyte strains as average or as elevated:

Table 2: Reference MICs used to analyse the dermatophyte MIC level observed in this study; []: Values in square brackets are tentative ECOFFs set by the EUCAST; ¹: Source: (European Committee on Antimicrobial Susceptibility Testing 2022); *: Determined using the CLSI broth microdilution method

Antifungal	Dermatophyte	Reference MIC [$\mu\text{g/mL}$]	Source
Amorolfine	<i>T. indotineae</i>	Tentative ECOFF: [≤ 0.5]	¹
Itraconazole	<i>T. indotineae</i>	Tentative ECOFF: [≤ 0.25]	¹
Miconazole	<i>T. interdigitale</i> <i>Trichophyton</i> spp.	Range: 0.5-8; MIC ₉₀ =8* Range: 0.25-0.5*	(Baghi et al. 2016) (Nizam et al. 2016)
Terbinafine	<i>T. indotineae</i> <i>T. mentagrophytes</i>	Tentative ECOFF: [≤ 0.125] Tentative breakpoint: ≥ 0.2	¹ (Nenoff et al. 2020)
Griseofulvin	<i>T. interdigitale</i>	Range: 0.5-4; MIC ₉₀ =2*	(Baghi et al. 2016)
Ciclopirox olamine	<i>T. mentagrophytes</i> / <i>interdigitale</i>	Range: 0.03-2*	(Shaw et al. 2020)
Fluconazole	<i>T. interdigitale</i>	Range: 2-64; MIC ₉₀ =64*	(Baghi et al. 2016)
Naftifine	<i>T. mentagrophytes</i>	Range: 0.03-1.0*	(Ghannoum et al. 2013)

Dermatophyte microdilutions were performed according to the protocol by (Arendrup et al. 2021). The tested antifungals were as follows: Amorolfine hydrochloride (Cat. No. not available, Acros Organics™/Thermo Fisher Scientific, Waltham, Massachusetts, USA), itraconazole (Cat. No. 15279786, distributed by Acros Organics™/Thermo Fisher Scientific, Waltham, Massachusetts, USA), miconazole (Cat. No. ab143414, Abcam, Cambridge, UK), terbinafine hydrochloride (Cat. No. ab141975, Abcam, Cambridge, UK), griseofulvin (Cat. No. PHR1534, Supelco/Sigma-Aldrich, St. Louis, Missouri, USA), ciclopirox (Cat. No. PHR1920, Supelco/Sigma-Aldrich, St. Louis, Missouri, USA), fluconazole (Cat. No. D212021/PF00345508-00/SB00957771, Pfizer, Brooklyn, New York City, New York, USA), and naftifine hydrochloride (Cat. No. HY-B0518A, MedChem Express, New Jersey, USA).

The testing ranges were set as follows: Amorolfine 0.002-4 µg/mL, itraconazole 0.016-32 µg/mL, miconazole 0.016-32 µg/mL, terbinafine 0.016-32 µg/mL, griseofulvin 0.016-32 µg/mL, ciclopirox 0.032-64 µg/mL, fluconazole 0.125-256 µg/mL, and naftifine hydrochloride 0.016-8 µg/mL. The microdilution plate layout is depicted in Figure 3.

	1	2	3	4	5	6	7	8	9	10	11	12	
Amorolfine hydrochloride	A	0.002	0.004	0.008	0.016	0.032	0.064	0.125	0.25	0.5	1	2	4
Itraconazole	B	0.016	0.032	0.064	0.125	0.25	0.5	1	2	4	8	16	32
Miconazole	C	0.016	0.032	0.064	0.125	0.25	0.5	1	2	4	8	16	32
Terbinafine hydrochloride	D	0.016	0.032	0.064	0.125	0.25	0.5	1	2	4	8	16	32
Griseofulvin	E	0.016	0.032	0.064	0.125	0.25	0.5	1	2	4	8	16	32
Ciclopirox	F	0.032	0.064	0.125	0.25	0.5	1	2	4	8	16	32	64
Fluconazole	G	0.125	0.25	0.5	1	2	4	8	16	32	64	128	256
Naftifine hydrochloride	H	WK	WK	0.016	0.032	0.064	0.125	0.25	0.5	1	2	4	8

Figure 3: Layout of dermatophyte microdilution plates

Cycloheximide (Cat. No. 01810, Sigma-Aldrich/Merck, Darmstadt, Germany; Cat. No. A0879,0005, PanReac AppliChem/ITW Reagents, Glenview, Illinois, USA) and chloramphenicol (Cat. No. PHR1412, Supelco/Sigma-Aldrich, St. Louis, Missouri, USA; Cat. No. A1806,0025, PanReac AppliChem/ITW Reagents, Glenview, Illinois, USA) were used to render the microdilutions selective for dermatophytes.

The cycloheximide stock solution was prepared by dissolving cycloheximide powder in DMSO at a concentration of 100 mg/mL. The chloramphenicol stock solution was prepared by dissolving chloramphenicol powder in absolute ethanol at a concentration of 50 mg/mL. Both stock solutions were vortexed and filtered using a syringe-powered 0.22 µm Millex[®]-OR filter (Cat. No. SLGL0250S, Merck Millipore, Billerica, Massachusetts, USA). The finished stock solutions were stored at 4°C overnight or at -80°C long-term.

The antifungal stock solutions used for microdilutions were prepared by dissolving the corresponding antifungal powder in DMSO to reach the required stock concentration (200x of the highest concentration in the microdilution plate). All stock solutions were stored at -80°C between uses.

To generate microdilution plates, the antifungal stock solutions were diluted 1:100 in double-strength sterile RPMI 1640 (2% glucose). Growth control wells contained double-strength RPMI-1640 (2% glucose) with 1:100 DMSO (without antifungal). 100 µL of the 2×RPMI medium supplemented with the respective antifungal (DMSO for growth control wells) were pipetted into each well of an uncoated flat-bottom microdilution plate. One microdilution plate batch contained 50-100 plates. The prepared plates were stored at -80°C.

For antifungal susceptibility testing, clinical dermatophyte isolates were cultured on Sabouraud dextrose agar or malt extract agar at 25-28°C for approximately seven days to reach sufficient growth. Fungal material was harvested using a soaked swab, homogenized on the wall of a McFarland tube and then stirred into sterile distilled water (dH₂O, for injection purposes) supplemented with 0.1% Tween-20 until a homogenous suspension was reached. The suspension was vortexed, adjusted to 0.5 McFarland with dH₂O supplemented with 0.1% Tween-20, and diluted 1:10 with dH₂O. Then, the suspension was supplemented with cycloheximide and chloramphenicol to a concentration of 600 mg/L and 100 mg/L, respectively (2× final concentration). 100 µL of the final suspension were added to each well (1:2 dilution) of a pre-thawed microdilution plate.

To avoid evaporation, microdilution plates were incubated in a wet chamber at 25-28°C for 5 days. The results were read visually as well as with the SpectraMax M2 photospectrometer at 490 nm (software: SoftMax Pro 7.0), as stated in the publication by (Arendrup et al. 2021).

Since the values obtained by visual inspection seemed more accurate than the values obtained using the SpectraMax (due to clumping growth observed in some strains), the visual values were used for further analyses. The difference between these two reading methods were ≤ 2 twofold difference in titre.

The quality control strains *Aspergillus flavus* ATCC 204304, *Aspergillus flavus* CNM-CM1813, *Trichophyton interdigitale* SSI-9396/CCUG 74948, and *Trichophyton rubrum* SSI-7583/CCUG 74971 and their corresponding quality control MIC value sheets published by the EUCAST were used to monitor microdilution plate accuracy, as suggested by (Arendrup et al. 2021).

Viability controls/colony counts were performed according to (Arendrup et al. 2021) by diluting 10 μ L of the 1:10 inoculum suspension in 2 mL dH₂O. The suspension was vortexed thoroughly, and 100 μ L were spread on Sabouraud agar plates. Agar plates were sealed with parafilm and incubated at 25-28°C; colonies were counted after 5 days (dermatophytes) or after 2 days (*Aspergillus* quality control strains).

2.4 DNA Extraction

Since the best way of collecting fungal material from dermatophytes for DNA extraction purposes was not known, several methods were tested. First, cultures were swabbed with a swab soaked in dH₂O, which resulted in a relatively thin fungal suspension and low DNA yields.

Then, an inoculation loop or a scalpel was used to cut out pieces of mycelium, and the suspension was homogenized as much as possible using thorough vortexing. However, this method also resulted in a low DNA yield in addition to suboptimal 260/230 values (possibly due to components of the agar such as polysaccharides).

The third method consisted of flooding the agar plate with dH₂O and homogenizing the resulting suspension with glass beads. This method resulted in good DNA yields, but varying 260/230 ratios (possibly to due agar components being washed into the fungal suspension).

Finally, the dermatophytes strains were cultured in Sabouraud broth supplemented with 300 mg/L cycloheximide and 50 mg/L chloramphenicol to inhibit the growth of bacteria and other moulds. Dermatophyte strains in bouillon were cultivated at 25-28°C on a rotamix. Upon DNA

extraction, the bouillon was discarded, and the fungal material was washed twice using dH₂O. Following, the fungal material was spun down and transferred into the bead-beating tubes containing ceramic beads (1 mm diameter) using a disposable Pasteur pipette. This method resulted in satisfying DNA yields as well as 260/230 ratios.

To commence the DNA extraction, the fungal material was placed into 120 µL 10% SDS and 10 µL Proteinase K in bead-beating tubes to lyse the fungal cells, followed by a 30 minute-incubation at 65°C and bead-beating using the Homogenizer FastPrep (MP Biomedicals, Santa Ana, CA, USA). Then, 120 µL 5M NaCl and 65 µL 10% CTAB (65°C) were added to bind polysaccharides, followed by 1h of incubation and consequent bead-beating. To separate the DNA from proteins and lipids, 700 µL chloroform:isoamyl alcohol (24:1) were added, and the phases were separated by centrifuging the sample at 15000 rpm at 4°C for 5 minutes. The top layer (~600 µL) was transferred to a new 2 mL Eppendorf tube. DNA was precipitated by adding 225 µL 10M ammonium acetate, filling the Eppendorf tube to the rim with absolute ethanol and inverting the tubes carefully to mix the contents. The precipitation was performed overnight at -20°C, followed by centrifugation at 4°C, 15000 rpm for 10 minutes. Several precipitation methods (5M ammonium acetate/NaCl, isopropanol) were tested, and this method proved most successful. The supernatant was discarded, and the pellet was washed twice with ice-cold ethanol, air-dried, eluted in 30 µL buffer EB (Cat. No. 19086, QIAGEN, Hilden, Germany). DNA samples were stored at -20°C. DNA extraction was performed based on a protocol by (Spettel et al. 2019, 2021).

DNA concentrations were measured using the Invitrogen™ Qubit® dsDNA High Sensitivity/HS (Cat. No. Q32854, ThermoFisher Scientific, Waltham, Massachusetts, USA) as well as the Broad Range/BR (Cat. No. Q32853, ThermoFisher Scientific, Waltham, Massachusetts, USA) Assay Kit according to manufacturer instructions. Briefly, the Qubit® dsDNA HS/BR Reagent was diluted 1:200 with the Qubit® dsDNA HS Buffer. 2 µL DNA were added to 198 µL of the working solution. Standards were prepared by adding 10 µL of Standard 1 or Standard 2 (respectively) to 190 µL working solution. All sample and standard tubes were vortexed for 2-3 seconds and incubated at room temperature for 2 minutes. Finally, the standard curve was constructed using Standard 1 and 2, and the samples were measured using the

Invitrogen™ Qubit® 2.0 fluorometer (ThermoFisher Scientific, Waltham, Massachusetts, USA).

DNA purity was assessed by pipetting 2 µL of each sample onto the pedestal of the Nanodrop™ 2000c spectrophotometer (ThermoFisher Scientific, Waltham, Massachusetts, USA), which was previously blanked with 2 µL buffer EB. Following, the A260 and A280 values as well as the A260/A280 and A260/A230 ratios were measured using the NanoDrop 2000 software.

2.5 Induction of *In Vitro* Resistance

In vitro resistance induction has been performed using *Candida* (Barker et al. 2004) and *Aspergillus* (Marques De Araujo et al. 2019). This study aimed to induce resistance mechanisms in dermatophytes using a similar method. This induction trial was performed in order to compare antifungal susceptible to -resistant strains without the need for an external reference sequence potentially introducing errors due to a slightly different *ERG1* genotype.

Four (previously determined) terbinafine- and naftifine susceptible clinical dermatophyte isolates and one susceptible EUCAST quality control strain (*T. rubrum*, SSI-7583/CCUG 74971) were cultured in microdilution plates prepared in 2.3 (culture conditions: wet chamber, 25-28°C) or several weeks. Dermatophyte growth was assessed weekly to bi-weekly, and whenever macroscopic growth was visible, the well contents were resuspended and 100 µL were transferred into the next well featuring the two-fold antifungal concentration. Additionally, the last well with growth was regularly transferred to a new plate to avoid the breakdown of the antifungal over time.

The induction was performed until growth was visible in concentrations far beyond the MIC values previously observed in these strains during the experiment. The final antifungal concentrations were as follows: $c_{\text{final_amorolfine}} = 2\text{-}4 \mu\text{g/mL}$, $c_{\text{final_itraconazole}} = 1\text{-}8 \mu\text{g/mL}$, $c_{\text{final_miconazole}} = 1\text{-}16 \mu\text{g/mL}$, $c_{\text{final_terbinafine}} = 1\text{-}2 \mu\text{g/mL}$, $c_{\text{final_griseofulvin}} = 2\text{-}32 \mu\text{g/mL}$, $c_{\text{final_ciclopirox}} = 0.5\text{-}4 \mu\text{g/mL}$, $c_{\text{final_fluconazole}} = 16\text{-}256 \mu\text{g/mL}$, $c_{\text{final_naftifine}} = 0.5\text{-}1 \mu\text{g/mL}$. The final concentrations varied depending on the antifungal, as the starting MIC values as well as the growth rate also varied depending on the antifungal.

The induced strains were then transferred to malt dextrose agar plates without added antifungals for one passage to determine if the resistance was transient (only present in high antifungal

concentrations, subsiding in the absence of antifungal exposure) or permanent. After sufficient fungal growth on the agar plates, the MIC was determined using the EUCAST microdilution method (see 2.3) once more.

2.6 DermaGenius[®] real-time PCR

To assess the performance and feasibility of the DermaGenius[®] Resistance Multiplex real-time PCR kit (Cat. No. PN-303, PathoNostics, Maastricht, Netherlands) for the routine determination of *ERGI* F397L and L393F resistance mutations, the results of this kit were compared to next-generation sequencing results for all dermatophyte strains used in this thesis.

DNA extraction was performed using the PathoNostics Extraction kit (Cat. No. PN-502, PathoNostics, Maastricht, Netherlands) according to manufacturer instructions. Briefly, a piece of mycelium the size of a small inoculation loop was added to 100 μ L solution A pre-mixed with 5 μ L internal control. The suspension was incubated at 98°C for 10 minutes and spun down. Then, 14 μ L solution B were added and the tube was vortexed thoroughly for 5 seconds. Finally, the sample was centrifuged for 1 minute at 10658 \times g (~13 000 rpm) and 50 μ L of the supernatant (final DNA sample) was transferred to a new Eppendorf tube. One extraction control containing only the reagents (no fungal material) was performed for each extraction. DNA samples were stored at 4°C short-term, or at -20°C long-term.

The PCR reactions were pipetted according to the manufacturer's instructions (see Table 3). The PCR mix was prepared for a slightly larger number of reactions (+10%), and one positive control (Resistance Positive Control, included in the kit) as well as one negative control (dilution buffer) and one extraction control were included in each run. The run was performed on the MIC qPCR cycler (bio molecular systems/BMS, Queensland, Australia) using the DermaGenius[®] PCR protocol in Table 4 in the micPCR software, v2.9.0. As the DermaGenius[®] Resistance PCR only uses one master mix to detect the SQLE target mutations L393F, F397L as well as the most common dermatophyte species, only one set of PCR reactions was prepared.

Table 3: Components of the DermaGenius® PCR reaction

Component	Volume/reaction
DermaGenius® Resistance PCR mix	10 µL
Taq polymerase	1.5 µL
Dilution buffer	8.5 µL
Total volume of master mix	20 µL
(+DNA	5 µL)

Table 4: DermaGenius® PCR protocol

	Step	Temperature	Duration	Cycles
Initial denaturation	<i>Taq</i> activation	95°C	120 s	1
Cycling	Denaturation	96°C	15 s	45
	Annealing/Extension	55°C	60 s	
Melt	Green	96°C; 45°C; Melt 45°C →85°C	120 s; 90 s; 0.3°C/s	1
	Yellow	96°C; 45°C; Melt 45°C →85°C	120 s; 90 s; 0.3°C/s	1
	Orange	96°C; 45°C; Melt 45°C →85°C	120 s; 90 s; 0.3°C/s	1

Since some strains could not be identified using the DermaGenius® Resistance kit (no melt curve), these strains and the strains not classified as “*Trichophyton mentagrophytes/interdigitale*” or “*Trichophyton mentagrophytes Type 4*” by the Resistance kit were re-analysed using the DermaGenius® 3.0 Complete Multiplex real-time PCR kit (Cat. No. PN-402, PathoNostics, Maastricht, Netherlands). As the DNA extraction method is the same for all DermaGenius® PCR kits, the previously extracted DNA samples were reused. All PCR components except the PCR mix are the same in the DermaGenius® 3.0 kit as in the resistance

kit (see Table 3). The DermaGenius[®] 3.0 uses three different PCR mixes: Two mixes differentiate between several fungal genera and species, and the third mix is a pan-dermatophyte PCR to evaluate the presence of dermatophyte DNA in the sample. In this thesis, only the first two master mixes were used, which means that all tested samples were set up in duplicate. The PCR protocol is the same as in the DermaGenius[®] Resistance kit (see Table 4).

2.7 PCR Design

The PCR and the library prep were performed according to the “16s metagenomic sequencing library preparation” guide for the MiSeq[™], provided by Illumina. Since this guide is specialized for the *16S* sequence found in bacteria and we aimed to analyse the *ITS2* region and the *ERG1* gene of fungi, the PCR conditions were adapted as follows.

The maximum sequencing length for the Illumina MiSeq[™] is 500 bp. Since most publications perform Sanger sequencing of the whole *ERG1* and *ITS2* genes with amplicon sizes of 600 bp up to >1 kb, most published primers did not qualify for our purpose. The chosen *ITS2* primer combination (see Table 5) has been reported to create an amplicon with a length of 400 bp. (Turenne et al. 1999) The *ERG1* mutation hotspot primers SQEL397S (binding locus 1049-1067 bp) and SQEL397R (binding locus 1424-1443 bp) were selected as they reportedly generate an amplicon with a length of max. 394 bp. (Kano et al. 2021) One wobble base was added to each of the *ERG1* primers to account for species-specific differences in the *ERG1* gene. Furthermore, the Illumina overhang adapters were added to each primer to ensure compatibility with the Illumina system (specifically with the index and sequencing adapters).

The melting temperature of all primers was analysed using the IDT OligoAnalyzer[™] tool. As all primers had a different melting temperature, a universal melting temperature of 60°C was chosen. The PCR conditions were verified in a test run with a small number of dermatophyte DNA samples prior to the main experiment. Furthermore, the possibility of multiplexing the *ITS2* and *ERG1* PCR was assessed.

Table 5: Primers and Illumina overhang adapters for the specific PCR of dermatophytes

Gene	Primer	Sequence (5'→3')	Melting temp. [°C]	Source
Illumina overhang adapter fw		TCGTCGGCAGCGTCAGATGTGTATAAGAGACAG		
Illumina overhang adapter rv		GTCTCGTGGGCTCGGAGATGTGTATAAGAGACAG		
<i>ITS2</i> fw	ITS86F	GTGAATCATCGAATCTTTGAAC	59.5	(Turenne et al. 1999)
<i>ITS2</i> rv	ITS4	TCCTCCGCTTATTGATATGC	61	(White et al. 1990)
<i>ERG1</i> fw	SQEL397S	GTTTRACTGGTGGCGGTATG	61.6/63.8	Adapted from (Kano et al. 2021)
<i>ERG1</i> rv	SQEL397R	GCTACGGAGTAAAAATGYCG	60.1/62.5	Adapted from (Kano et al. 2021)

2.8 PCR, Library Prep and NGS

The KAPA HiFi HotStart ReadyMix (Cat. No. KK2602, Roche, Basel, Switzerland) was used for both the specific PCR as well as the index PCR since it is a high-fidelity polymerase (1 error in 3.6×10^6 nucleotides) suitable for sequencing library amplification (according to the manufacturer's website) and since it is indicated by the Illumina guide.

The previously extracted DNA was transferred to a PCR plate and diluted to 5 ng/ μ L using buffer EB (Cat. No. 19086, QIAGEN, Hilden, Germany). The master mix for the specific *ERG1/ITS2* PCR was prepared in a separate PCR plate according to Table 6. Following, 2.5 μ L DNA (5 ng/ μ L) were transferred to each well the PCR plate containing 22.5 μ L master mix. The PCR was performed according to a newly established protocol for this primer combination (see Table 7), which was tested previously (see 3.5). The PCR plates containing the PCR products were stored at 4°C.

PCR success was verified using gel electrophoresis with a 1.8% agarose gel at 120V for 30 minutes (big gel) and at 60-80 V for >1 hour (small gel, to reach optimal resolution). The agarose gel was stained using GelRed® Nucleic Acid Stain, 10 000X (Cat. No. 41002, Biotium, Fremont, California, USA). The Invitrogen™ 100 bp DNA ladder (Cat. No. 15628019, ThermoFisher Scientific, Waltham, Massachusetts, USA) was used for amplicon size reference. Samples were loaded using the Gel Loading Dye Purple (6X) (Cat. No. B7024S, New England Biolabs, Ipswich, Massachusetts, USA).

Table 6: PCR components for the dermatophyte PCR

	Component	Volume/reaction
Specific <i>ERG1/ITS2</i> Multiplex PCR	KAPA HiFi HotStart ReadyMix	12.5 µL
	PCR H ₂ O	6 µL
	Primer ITS86F, 10 µM	1 µL
	Primer ITS4, 10 µM	1 µL
	Primer SQEL397S, 10 µM	1 µL
	Primer SQEL397R, 10 µM	1 µL
	Total volume	22.5 µL
	(+DNA, 5 ng/µL)	2.5 µL)
Illumina Index PCR	Master Mix	
	KAPA HiFi HotStart ReadyMix	25 µL
	PCR H ₂ O (10 µl/sample)	10 µL
	Nextera Index Primer	5 µL
	Nextera Index Primer	5 µL
	Total volume	45 µL
	(+ Purified amplicons from specific PCR	5 µL)

Table 7: PCR programs for the *ERG1/ITS2* and the Illumina index PCR

	Step	Temperature	Duration	Cycles
Specific <i>ERG1/ITS2</i> Multiplex PCR	Initial denaturation	95°C	3 min	1
	Denaturation	98°C	20 s	30
	Annealing	60°C	30 s	
	Extension	72°C	30 s	
	Final extension	72°C	5 min	1
Illumina Index PCR	Initial denaturation	95°C	3 min	1
	Denaturation	98°C	30 s	8
	Annealing	55°C	30 s	
	Extension	72°C	30 s	
	Final extension	72°C	5 min	1

After the specific PCR, the amplicons were purified according to the PCR Clean-Up 1 procedure specified in the Illumina protocol. Briefly, the plate containing the products of the specific PCR was spun down. 24 μ L AMPure XP beads (Cat. No. A63881, Beckman Coulter, Brea, California, USA) at room temperature were added to each well and the well contents were resuspended thoroughly to bind the amplified DNA to the magnetic beads. The plate was incubated at room temperature for 5 minutes and then transferred to a magnetic stand until the beads collected at the rim of the well and the supernatant was clear (~3 minutes). Following, the supernatant consisting of the reagents of the specific PCR was discarded, the DNA attached to the beads was washed twice with 200 μ L 80% ethanol in DEPC H₂O and air-dried. The plate was removed from the magnetic stand, and the beads were resuspended in 52.5 μ L buffer EB (Cat. No. 19086, QIAGEN, Hilden, Germany) and incubated for 2 minutes at room temperature to elute the DNA. The plate was placed on the magnetic stand again, and the supernatant containing the purified DNA was transferred to a new plate. The “empty” beads were discarded, and the purified DNA was stored at 4°C.

The index PCR was performed using 5 μ L of the purified amplicons, 35 μ L master mix and 5 μ L each of two distinct index primers from the Nextera XT v2 Index kit Set A (Cat. No. FC-131-2001, Illumina, San Diego, California, USA) per well (see Table 6). As each well/sample

featured a distinct index primer combination (see Figure 4), these primers served the purpose of barcoding/identifying the samples during the NGS run when all samples were pooled. The index PCR protocol is depicted in Table 7.

ERG1.ITS Dermatophyten Plate 1												
	1	2	3	4	5	6	7	8	9	10	11	12
A	F1114 S502 N701	F1234 S502 N702	F1318 S502 N703	T1_28 S502 N704	T1_46 S502 N705	T1_115 S502 N706	T1_A11 S502 N707	D31 S502 N710	D74 S502 N711	D163 S502 N712	D187 S502 N714	D217 S502 N715
B	F1213 S503 N701	F1235 S503 N702	F1326 S503 N703	T1_29 S503 N704	T1_47 S503 N705	T1_117 S503 N706	T1_A12 S503 N707	D35 S503 N710	D75 S503 N711	D168 S503 N712	D195 S503 N714	D221 S503 N715
C	F1214 S505 N701	F1252 S505 N702	F1329 S505 N703	T1_30 S505 N704	T1_48 S505 N705	T1_125 S505 N706	T1_A13 S505 N707	D40 S505 N710	D113 S505 N711	D172 S505 N712	D198 S505 N714	D235 S505 N715
D	F1215 S506 N701	F1256 S506 N702	F1330 S506 N703	T1_31 S506 N704	T1_102 S506 N705	T1_126 S506 N706	T1_A23 S506 N707	D46 S506 N710	D116 S506 N711	D173 S506 N712	D200 S506 N714	D241 S506 N715
E	F1216 S507 N701	F1257 S507 N702	F1333 S507 N703	T1_32 S507 N704	T1_103 S507 N705	T1_A3 S507 N706	D5 S507 N707	D48 S507 N710	D117 S507 N711	D176 S507 N712	D204 S507 N714	D243 S507 N715
F	F1217 S508 N701	F1258 S508 N702	F1366 S508 N703	T1_43 S508 N704	T1_108 S508 N705	T1_A4 S508 N706	D11 S508 N707	D63 S508 N710	D145 S508 N711	D180 S508 N712	D211 S508 N714	D244 S508 N715
G	F1223 S510 N701	F1303 S510 N702	T1_6 S510 N703	T1_44 S510 N704	T1_109 S510 N705	T1_A9 S510 N706	D12 S510 N707	D68 S510 N710	D146 S510 N711	D183 S510 N712	D214 S510 N714	D247 S510 N715
H	F1224 S511 N701	F1313 S511 N702	T1_27 S511 N703	T1_45 S511 N704	T1_112 S511 N705	T1_A10 S511 N706	D13 S511 N707	D71 S511 N710	D150 S511 N711	D185 S511 N712	D216 S511 N714	D250 S511 N715

ERG1.ITS Dermatophyten Plate 2												
	1	2	3	4	5	6	7	8	9	10	11	12
A	D265 S502 N716	D297 S502 N718	F1366 S502 N719	D283 S502 N720								
B	D267 S503 N716	SSI-9363 S503 N718	D270 S503 N719	NK_PCR1.1 S503 N720								
C	D278 S505 N716	SSI-7583 S505 N718	D271 S505 N719	NK_PCR1.2 S505 N720								
D	D282 S506 N716	D301 S506 N718	D274 S506 N719	NK_PCR2 S506 N720								
E	D285 S507 N716	D302 S507 N718	D288 S507 N719									
F	D286 S508 N716	D303 S508 N718	D266 S508 N719									
G	D292 S510 N716	D304 S510 N718	D290 S510 N719									
H	D293 S511 N716	D305 S511 N718	D280 S511 N719									

Figure 4: Illumina plate layout featuring the index primer combinations

Following the index PCR, the amplicons were purified in the PCR Clean-Up 2, which was performed in the same way as the Clean-Up 1 but with 28 μ L AMPure XP beads per well. Then, the DNA was quantified using the Invitrogen™ Qubit® dsDNA HS Assay Kit (Cat. No. Q32854, ThermoFisher Scientific, Waltham, Massachusetts, USA). The samples were diluted

to 4 nM using buffer EB (Cat. No. 19086, QIAGEN, Hilden, Germany) and 5 μ L of each sample were pooled into a DNA LoBind[®] Eppendorf tube (5 μ L/sample) and vortexed thoroughly.

The purified and diluted amplicons were denatured by adding 5 μ L 0.2 M NaOH to 5 μ L DNA and incubating the mixture at room temperature for 5 minutes. Following, the denatured 4 nM library was first diluted to 20 pM and then to 5 pM in HT1. Finally, 60 μ L PhiX (previously diluted to 5 pM in HT1) was added to 540 μ L of 5 pM library to reach a concentration of 10% PhiX. Aside from the denaturation using NaOH and DNA, all reagents were kept on ice at all times.

The NGS run was performed on the Illumina MiSeq[™] using a PE-Nano MiSeq[®] Flow Cell (Cat. No. 15035217, Illumina, San Diego, California, USA) and the corresponding reagents from the MiSeq[®] v2 Reagent Kit and Reagent Nano Kit v2 (Cat. No. 15033625 and 15036714, Illumina, San Diego, California, USA). The samples were read in paired-end mode.

Using the raw NGS data, *ERGI* and *ITS2* sequences were assembled *de novo* using the SPAdes genome assembler. Briefly, all reads containing the respective *ITS2* or *ERGI* primer sequences were compiled into a file, and the primer sequences were removed using Cutadapt. The DADA2 pipeline was used to extract the amplicon sequence variants (ASVs), which outline the specific genotype of each strain. The most common *ERGI* ASV was blasted using the NCBI BLAST and the resulting sequence with a coverage of 100% within the sequenced region (*T. interdigitale*, accession no. OM313312.1) was used as a reference sequence for the variant calling of all strains. This comparison resulted in *ERGI* genotype groups, which each had a unique ASV.

The variant-calling pipeline consisted of the tools Trimmomatic (trimming the low-quality bases <Q30), Bowtie (aligning the reads to the reference sequence), samtools (sorting and indexing the data), VarScan (detecting variants/mutations in relation to the reference sequence), and SnpEff (annotating the variants/mutations to their respective locations).

Furthermore, the ASV sequences were compared to the UNITE database (using DADA2) as well as the NCBI BLAST database. The *ITS2* sequences were also manually compared to the Mycobank database to receive a secondary species identification. The *ERGI* ASVs were not

compared to the UNITE or the Mycobank databases, as these databases only contain taxonomic markers. Only results with a coverage of 100% were considered as matches.

Additionally, a list of the specific nucleotide variants was generated for *ERG1*. These variants were filtered for coding mutations resulting in changes in the amino acid sequence of the squalene epoxidase protein. All coding mutations and their corresponding changes in the amino acid sequence were analysed by hand to identify potential resistance mutations as well as non-causal variants.

Mutations featuring a low frequency and sequencing depth (potential bioinformatic contaminations) were filtered. If a mutation was only present in strains with terbinafine/naftifine MIC values within the normal distribution or present in strains with normal as well as elevated MIC values, it was deemed non-causal for terbinafine resistance. However, if a mutation was only present in strains with elevated terbinafine/naftifine MIC values, it was termed as potentially causal (resistance) mutation.

3 Results

3.1 Culture Morphology

As visible in Figure 5, macroscopic culture morphology between strains of *Trichophyton mentagrophytes* and *Trichophyton interdigitale* was vastly different. The surface of the colonies appeared cottony in some strains, and powdery in others. While some strains maintained a smooth surface profile, others bulged out of the agar. And some isolates featured several rings while others did not. The top culture pigmentation ranged from white to cream colour and in one case, it was even a light pink colour. Bottom pigmentation ranged from a light cream colour to a dark brown and in some cases a vibrant red.

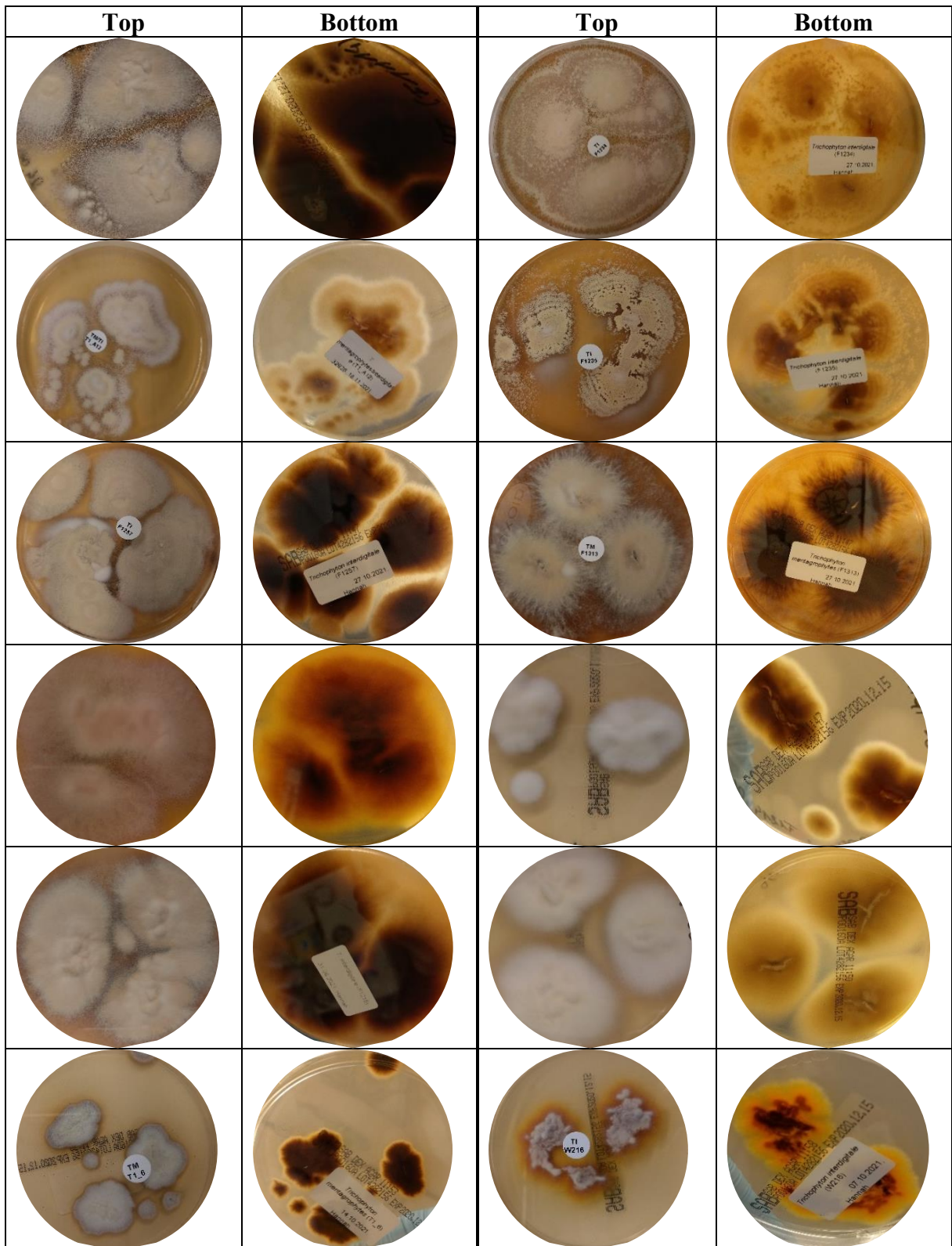


Figure 5: Macroscopic culture morphology of strains confirmed as part of the *T. mentagrophytes/interdigitale* species complex using NGS (see 3.6)

The microscopic morphology of strains within the *T. mentagrophytes/interdigitale* species complex was observed using the lactophenol blue staining method. As visible by the examples in Figure 6, strains of this species featured an abundance of spherical microconidia (indicated by purple arrows) arranged in clusters around hyphae. Furthermore, cylindrical macroconidia (indicated by yellow arrows) could be found in D301 and spiral hyphae (green arrows) could be found in cultures of D301 and F1366. Interestingly, in the isolates F1114 and F1366, several large, spherical structures (red arrows) were found. Due to the morphology of the microconidia and macroconidia as well as the presence of spiral hyphae, the observed strains might belong to the *T. mentagrophytes/interdigitale* complex (see (Campbell et al. 2013)).

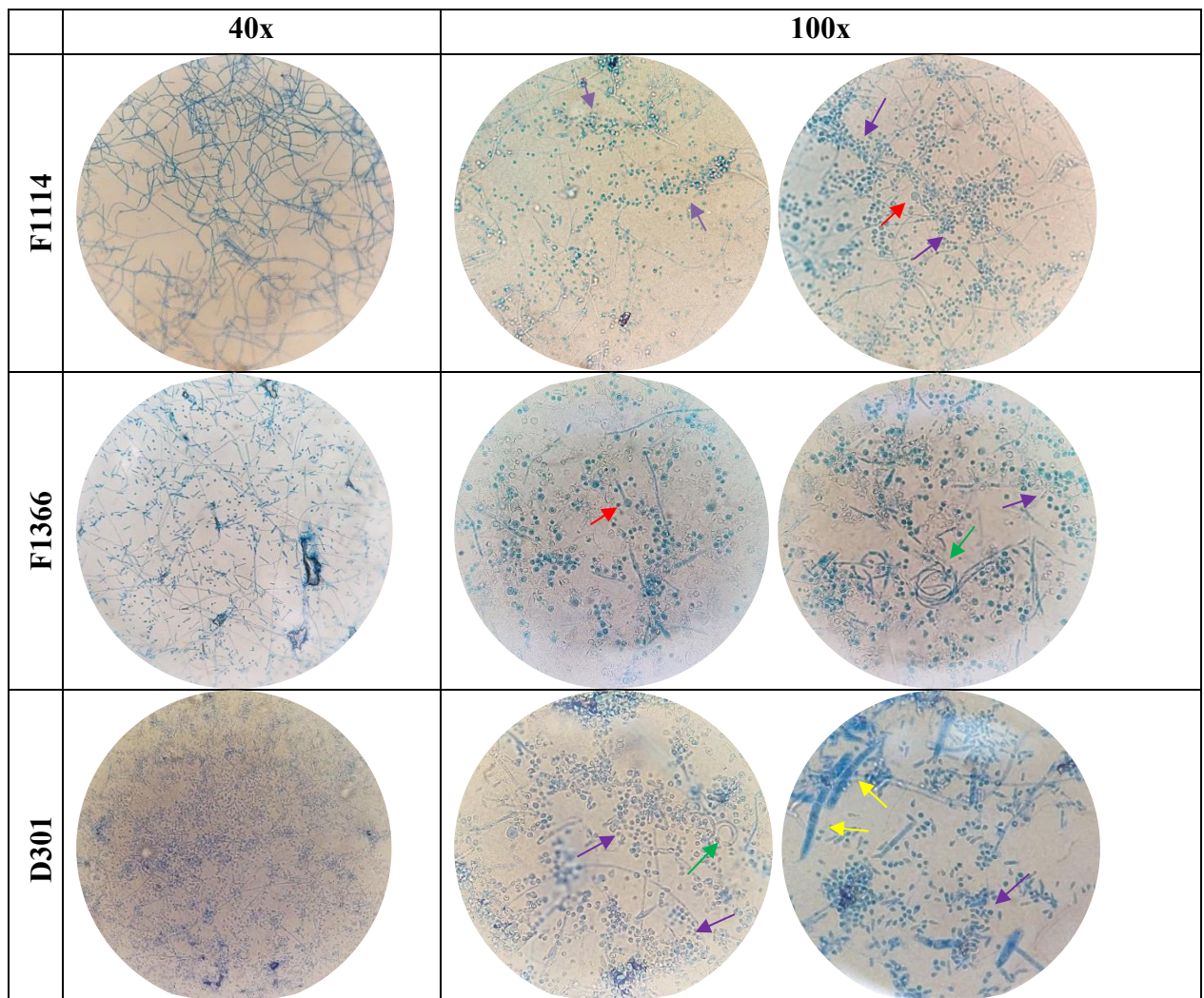


Figure 6: Lactophenol blue staining of strains confirmed as part of the *T. mentagrophytes/interdigitale* species complex, 40x and 100x magnification (light microscopy); purple arrows: microconidia, yellow arrows: macroconidia, green arrows: spiral hyphae, red arrows: spherical structures

3.2 Microdilutions

The results of the antifungal susceptibility testing are visible in Figure 7. The MIC values of amorolfine, itraconazole, miconazole, griseofulvin and fluconazole appear to be normally distributed as expected.

Amorolfine MIC values ranged between 0.008 µg/mL and 0.5 µg/mL. As the ECOFF is at a MIC of 0.5 µg/mL and no strains with MIC levels significantly above this distribution (outliers) were visible, all strains included in this study were classified as susceptible to amorolfine.

Itraconazole MIC values ranged between <0.016 µg/mL and 1 µg/mL. Since the ECOFF for itraconazole is 0.25 µg/mL, it could be argued that all isolates featuring a higher MIC value are resistant to itraconazole. However, since all MIC values fall into a normal distribution and no outliers are visible, isolates with a MIC \geq 0.25 µg/mL were still classified as susceptible to itraconazole.

Similar to itraconazole, miconazole MIC values ranged from <0.016 µg/mL to 2 µg/mL. No outliers were visible, and all isolates were classified as susceptible to miconazole.

Terbinafine MIC values did not show a normal distribution. This is most likely due to the design of the microdilution plate, as even the lowest terbinafine concentration in the plate is higher than the MIC value of most dermatophyte strains used in this study (future studies might therefore improve the design of the microdilution plate used in this study). Terbinafine MIC values were measured between <0.016 µg/mL and 4 µg/mL. However, the vast majority of samples feature MIC levels of \leq 0.032 µg/mL, and the terbinafine ECOFF is placed at 0.125 µg/mL (see Table 1). The strains D301 and F1366 featured MIC values of 0.5 µg/mL and 4 µg/mL, respectively. Due to the large distance between the MIC values of most samples and these outliers as well as their MIC placement above the ECOFF, these two isolates were termed terbinafine resistant while all other isolates were classified as susceptible. The sample D301 was a strain sent by NEQAS, while the isolate F1366 was a clinical patient isolate.

Griseofulvin MIC values were normally distributed between 0.064 µg/mL and 4 µg/mL. As no outliers were found, all isolates were categorized as susceptible to Griseofulvin.

Ciclopirox MIC values showed no normal distribution. All analysed strains featured a ciclopirox MIC of either 0.5 µg/mL (55 isolates) or 1 µg/mL (51 isolates). As these values are

only one twofold titre difference apart and no outliers were present, all strains were categorized as susceptible to ciclopirox.

Fluconazole MIC values were normally distributed between the wide range of 1 µg/mL and 256 µg/mL. Even though no outliers were found, the MIC values of this particular antifungal are very high for all tested isolates. Therefore, it is likely not the most effective treatment option against strains of the *T. mentagrophytes/interdigitale* species complex.

Similar to terbinafine, naftifine MIC values are likely normally distributed but seem to be cut off at the lower border of the test range. Naftifine MIC values range between <0.016 µg/mL and >8 µg/mL, though most values lie between <0.016 µg/mL and 0.064 µg/mL. Two outliers are visible at 0.5 µg/mL and >8 µg/mL. These outliers belong to the samples D301 and F1366, respectively. As there is a large (≥ 6 -fold difference in titre) difference between the MIC values of most samples and these outliers, these samples were classified as resistant to naftifine. Since these isolates feature a resistance to naftifine as well as terbinafine, they were termed cross-resistant to allylamines based on the microdilution results.

All ECOFF values featured in Figure 7 are taken from (European Committee on Antimicrobial Susceptibility Testing 2022) and are specified for *Trichophyton indotineae*. No verified ECOFF values were available for *Trichophyton mentagrophytes* or *Trichophyton indotineae*. No clinical breakpoints were available for any dermatophyte species.

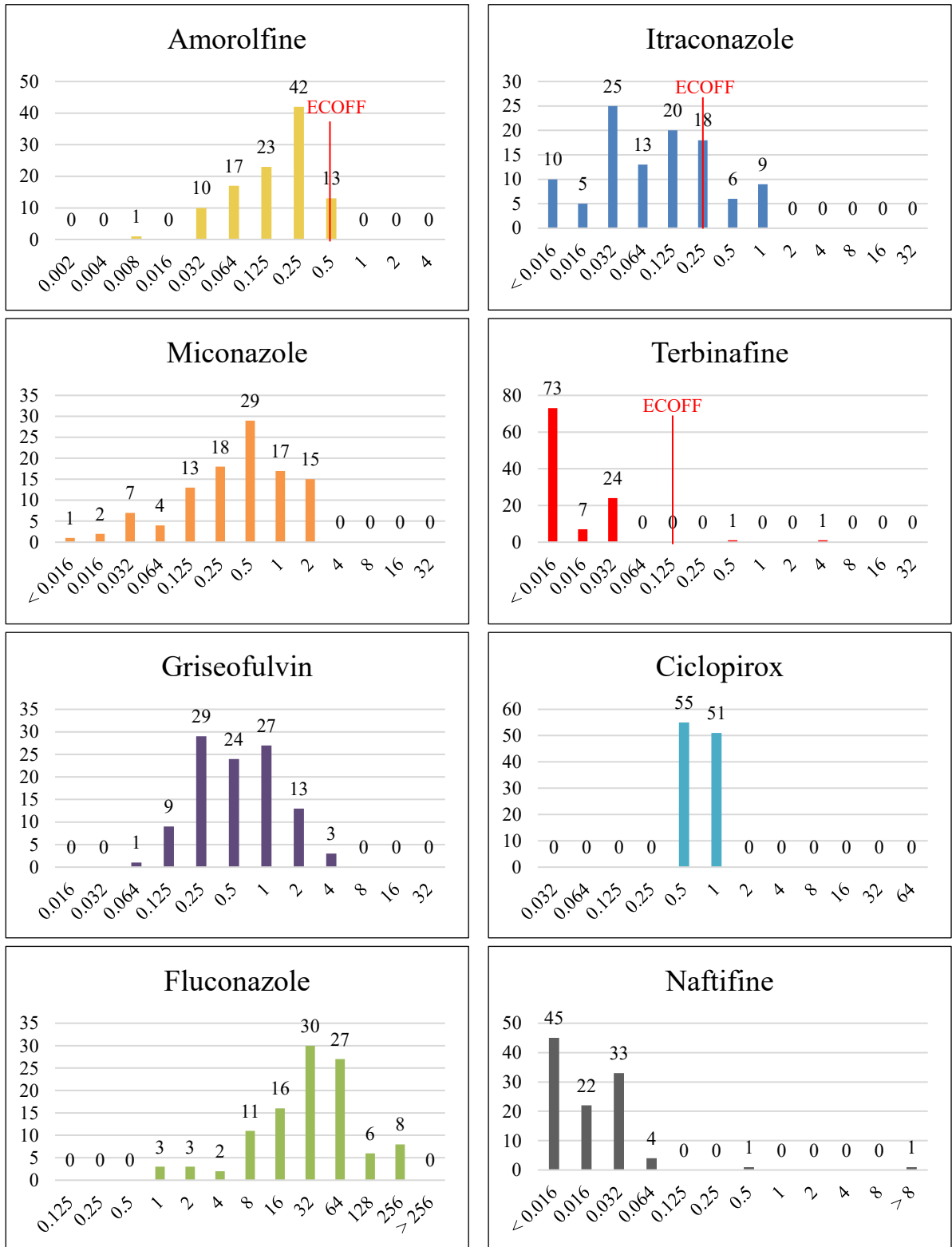


Figure 7: Minimum inhibitory concentration distributions of commonly used antifungals against strains of the *T. mentagrophytes/interdigitale* species complex; ECOFF values are taken from (European Committee on Antimicrobial Susceptibility Testing 2022) for *Trichophyton indotineae*

3.3 Induction of *In Vitro* Resistance

Induction of *in vitro* resistance was attempted by passaging five susceptible strains in increasing concentrations of commonly used antifungals. Compared to microdilutions where growth can be assessed after 5 days, dermatophyte strains during induction could only be transferred into the well every 1.5 to two weeks. This decrease in growth is likely due to the increased antifungal concentration, which at least partly inhibits fungal growth and/or metabolism.

As visible in Figure 8, dermatophyte strains grew densely and homogeneously prior to sub-cultivation in increased antifungal concentrations. After a few passages, the macroscopic morphology began to change and small, irregularly shaped aggregates, which increased as induction progressed, appeared. It is thought that this aggregation is done to form a physical barrier against the antifungal.



Figure 8: Dermatophyte growth before (left) and during/after (right) induction of *in vitro* resistance; changes in growth pattern applicable for all strains (n=5)

However, when cultures post-induction were seeded onto Sabouraud and malt extract agar plates, most strains did not grow – even after several weeks of incubation. The few strains which did grow post-exposure did not show significantly increased MIC values when re-tested using EUCAST microdilutions. The temporary nature of this antifungal resistance could be due to several factors: 1) The antifungal resistance was caused by cell aggregation, which was compromised during the transfer to new microdilution plates, 2) the antifungals used for resistance induction degraded over time despite the countermeasures, leading to a failure of resistance induction, 3) the antifungal resistance was caused by a transient upregulation in cellular stress response-, drug metabolism- or -efflux genes instead of fixed target resistance mutations, and 4) the induction of *in vitro* resistance promoted the formation of persister cells,

which are able to survive in high antifungal concentrations but resume growth and return to their susceptible state once the antifungal agent is removed. (Hazen 2000, Galdiero et al. 2020, Pires et al. 2021)

Due to these results, the induction of *in vitro* resistance to assess the development of resistance mutations was not further pursued.

3.4 DermaGenius[®] real-time PCR

To validate the PathoNostics DermaGenius[®] Resistance Multiplex real-time PCR kit, the dermatophyte species and *SQLE/ERG1* genotype of all samples was assessed using this kit. For samples where no species could be determined using the Resistance kit or where the result was not *Trichophyton interdigitale/mentagrophytes* or *Trichophyton mentagrophytes* Type IV, secondary analysis was performed using the DermaGenius[®] 3.0 Complete Multiplex real-time PCR kit (Cat. No. PN-402, PathoNostics, Maastricht, Netherlands). These kits can determine some dermatophyte species and potential *SQLE/ERG1* mutations using melting curve analysis (see Figure 9). Thresholds set by the program were checked and corrected manually if needed.

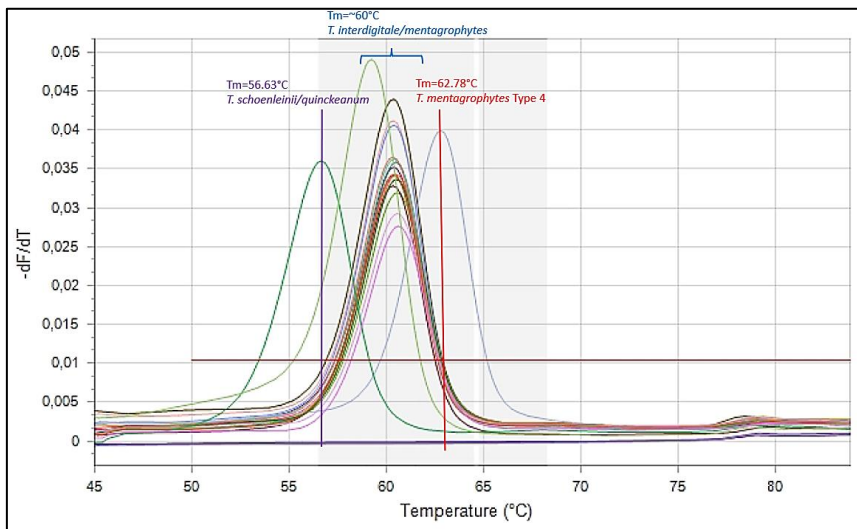


Figure 9: Species identification of dermatophyte strains using melting curve analysis (PathoNostics[®] DermaGenius[®] Resistance Multiplex real-time PCR kit)

Species identification using the DermaGenius[®] Resistance kit delivered results for 92 out of 106 isolates (see Table 8). Of the identified isolates, 82 were classified as *Trichophyton interdigitale/mentagrophytes*, 5 were identified as *Trichophyton schoenleinii/quinckeanum*, 2

each were identified as *Trichophyton mentagrophytes* Type IV and *Trichophyton rubrum/soudanense*, and one isolate was identified as *Trichophyton tonsurans*.

Table 8: Species identification of clinical dermatophyte isolates using the PathoNostics DermaGenius® Resistance Multiplex real-time PCR kit

Species (DermaGenius® Resistance)	Count of Species
<i>T. interdigitale/mentagrophytes</i>	82
Species not identified	14
<i>T. schoenleinii/quinckeanum</i>	5
<i>T. mentagrophytes</i> Type IV	2
<i>T. rubrum/soudanense</i>	2
<i>T. tonsurans</i>	1
Grand Total	106

The DermaGenius® 3.0 results are visible in Table 9: All 14 previously not identified isolates were identified as *Trichophyton benhamiae*, which is not included in the DermaGenius® Resistance kit. Additionally, the strains that were identified as another species than *T. mentagrophytes/interdigitale* using the DermaGenius® Resistance kit were re-identified using the DermaGenius® 3.0 kit. Strains of the species *Trichophyton rubrum/soudanense* (2 strains), *Trichophyton schoenleinii/quinckeanum* (1 strain) and *Trichophyton tonsurans* (1 strain) were identified as the same species by the DermaGenius® 3.0 kit. The four samples (F1330, D211, D301, D40) that were identified as differently were classified as *T. schoenleinii/quinckeanum* using the DermaGenius® Resistance kit, but as *T. interdigitale/mentagrophytes* using the DermaGenius® 3.0 kit.

Table 9: Species identification of clinical dermatophyte isolates using the PathoNostics DermaGenius® 3.0 Complete Multiplex real-time PCR kit

Species (DermaGenius® 3.0)	Count of Species
<i>T. benhamiae</i>	14
<i>T. interdigitale/mentagrophytes</i>	4
<i>T. rubrum/soudanense</i>	2
<i>T. schoenleinii/quinckeanum</i>	1
<i>T. tonsurans</i>	1
Grand Total	22

Furthermore, 2 out of 106 isolates were identified as having SQLE mutations in the L393F or F397L hotspots of the squalene epoxidase/*ERG1* gene by the DermaGenius® Resistance kit (see

Table 10). One of these strains (D301) was classified as *Trichophyton schoenleinii/quinckeanum* by the Resistance kit and as *T. interdigitale/mentagrophytes* by the DermaGenius® 3.0 kit, and the other strain (F1366) was identified as *Trichophyton interdigitale/mentagrophytes*. These strains also previously exhibited elevated MIC values and were classified as resistant (see section 3.2).

Table 10: SQLE/*ERG1* genotype identification of clinical dermatophyte isolates using the PathoNostics DermaGenius® Resistance Multiplex real-time PCR kit

SQLE Genotype	Count of SQLE Genotype
SQLE Mutant	2
SQLE Wildtype	104
Grand Total	106

3.5 PCR Design

Prior to starting the main experiment, the PCR conditions and primers were tested for their efficacy. As described in 3.4, some strains included in this sequencing run were likely not *T. mentagrophytes* or *T. interdigitale*. Therefore, the PCR conditions were tested for several dermatophyte species: *T. mentagrophytes/interdigitale* (D13), *T. rubrum* (F1396, D271, D288), *T. tonsurans* (D270, D274), *M. canis* (D266, D290), and *N. gypsea* (D280, D283). As visible in Figure 10, the *ERG1* PCR was successful for all strains except for *M. canis* and *N. gypsea* – likely due to a different *ERG1* genotype compared to the *Trichophyton* strains. The *ITS2* PCR was successful for all tested *Trichophyton* strains as well as *M. canis* and *N. gypsea*.

The multiplex PCR of *ERG1* and *ITS2* showed slightly thicker bands for all strains. However, due to the size of the gel, the resolution was not high enough to show the presence of two products. The gel of the repetition run (see Figure 11) features a better resolution and shows the presence of two separate products as well as their difference in size. The faint bands far below these PCR products are likely primer dimers. These results indicate that multiplexing both PCRs is a possibility to save reagents as well as time.

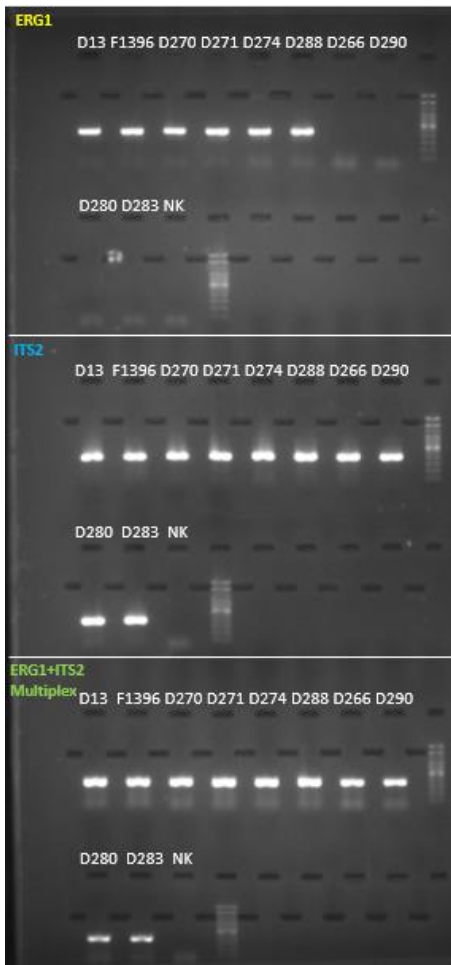


Figure 10: Results of the test run of the specific *ERG1/ITS2* PCR

3.6 PCR, Library Prep and NGS

The specific *ERG1/ITS2* PCR was successful for all samples except for T1_102, T1_103, T1_126, T1_A3, T1_A9, and D48 (see Figure 11A). The samples which did not show a PCR product were re-loaded (marked in red by “REP”, Figure 11B), but the second loading also resulted in a lack of bands. Therefore, the specific PCR of these samples was repeated, which resulted in a successful amplification as visible in Figure 11C. During *ITS2* sequencing (see 3.6), the samples T1_102, T1_103 and T1_A3 were confirmed to be *Trichophyton/Arthroderma benhamiae*, the sample T1_126 was confirmed to be *T. erinacei/benhamiae*, and the samples D48 and T1_A9 were confirmed to be *T. mentagrophytes/interdigitale*. Therefore, the PCR failure was likely not due to the species of the strain but rather a handling error.

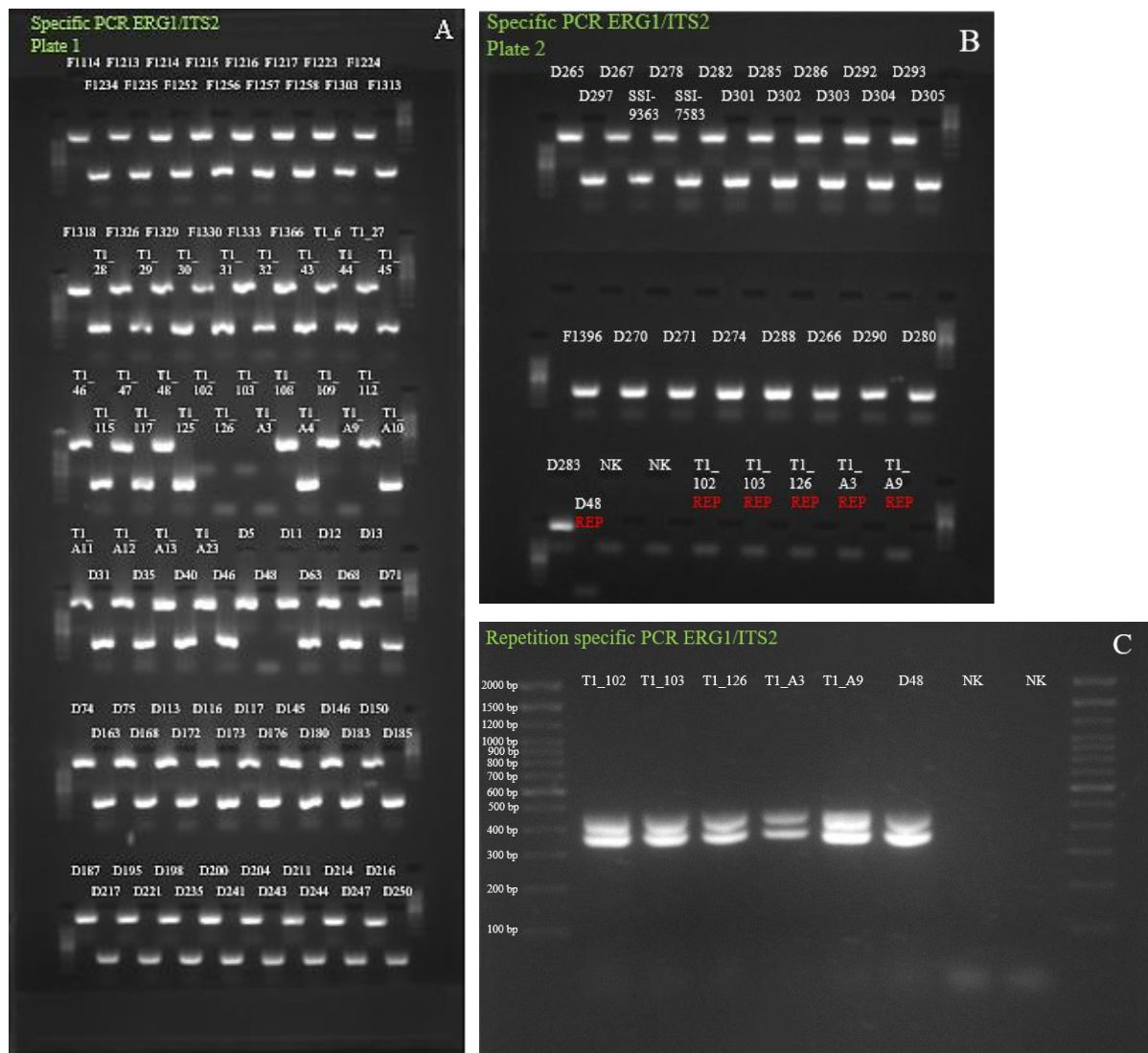


Figure 11: Results of the specific *ERG1/ITS2* PCR, main run; A: First run, plate 1; B: First run, plate 2 + second loading of samples without bands; C: Second run; repetition PCR of unsuccessfully amplified samples

Figure 12A depicts the run summary as well as the percentage of clusters passing the filter (89.48%), and the percentage of reads above the quality score of Q30 (one error in 1000 bp) of the NGS run. A quality score of 91.04%, as obtained in this study, is unusually high as NGS runs with ~80% of bases above Q30 are usually considered good quality.

Samples were read in paired-end mode (251 cycles per direction). The cluster density was at 1056 K/mm², which is on the higher end when compared with Illumina recommendations (800-1000 K/mm²). The cluster density is an essential feature of the sequencing run that describes

the spatial proximity of clusters of amplified DNA (each cluster being a multitude of clonal copies from a single DNA strand) generated during the sequencing run. As the fluorescence of each cluster is measured to determine the sequence of the fluorescence-labelled nucleotides, overclustering can lead to a lower quality, lower data output or even run failure. However, when taking the quality scores of this run (91.04% >Q30 and 89.48% of clusters passing the filter) into consideration, this NGS run featured excellent quality.

Figure 12B shows a thumbnail of the amplified clusters, while Figure 12C and Figure 12D show the varying quality scores during the run. The quality of the bases normally declines during the end of a run, which is why there are two decreases of base quality (at the end of the forward run and at the end of the reverse run).

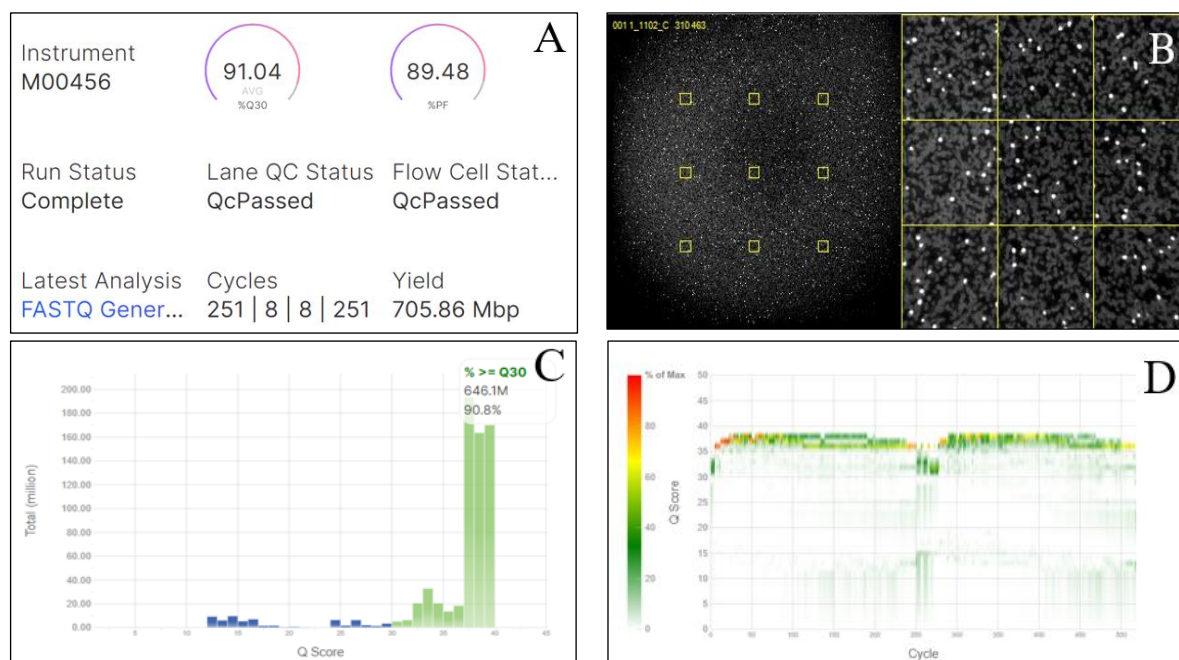


Figure 12: NGS run parameters; A: run summary, B: thumbnail of amplified clusters; C: quality scores; D: heatmap of quality scores throughout the run

Figure 13 features the results of the bioinformatic analysis of the *ITS2* NGS run. The obtained *ITS2* ASVs were blasted using the NCBI (Figure 13A), Mycobank (Figure 13B) and UNITE (Figure 13C) databases, and only results with a coverage of 100% were taken into consideration.

While the NCBI BLAST categorized 82 strains as *T. mentagrophytes/T. interdigitale*, Mycobank identified the same strains as *T. interdigitale* and the UNITE database classified

them as *T. mentagrophytes*. 9 samples identified as *T. benhamiae* by the NCBI BLAST were recognized as *Arthroderma (A.) benhamiae* by Mycobank, but only as members of *Trichophyton* spp. using the UNITE database. 8 samples classified as *T. mentagrophytes/interdigitale/indotineae* by the NCBI BLAST were only recognized as *T. mentagrophytes* by Mycobank and by the UNITE database. 3 samples identified as *T. mentagrophytes/benhamiae/europaeum/japonicum* by the NCBI BLAST were recognized as *Arthroderma (A.) benhamiae* by Mycobank, or as *A. benhamiae* by the UNITE database. 3 samples identified as *T. rubrum* by the NCBI and the Mycobank databases were identified as *T. violaceum* (2 strains) or as NA (1 strain) using the UNITE database. 2 samples identified as *T. erinacei/benhamiae* by the NCBI BLAST and as *T. erinacei* by Mycobank could only be classified as members of *Trichophyton* spp. using the UNITE database. 2 samples classified as *T. mentagrophytes/interdigitale/benhamiae/vanbreuseghemii* by the NCBI BLAST were categorized as *T. mentagrophytes/A. vanbreuseghemii/A. benhamiae* by Mycobank, but only as *T. mentagrophytes* using the UNITE database. 2 samples identified similarly as *T. mentagrophytes/interdigitale/benhamiae* and as *T. interdigitale/mentagrophytes/A. benhamiae* by the NCBI BLAST and Mycobank database were only identified as *T. mentagrophytes* using the UNITE database. Finally, one sample was identified as *T. tonsurans* using the NCBI BLAST and the UNITE database and as *T. equinum/tonsurans* using Mycobank.

The ITS2 NGS results align with the species identification provided with the PathoNostics DermaGenius® Resistance Multiplex and DermaGenius® 3.0 Complete Multiplex kits. 81 out of 82 Strains identified as *T. mentagrophytes/interdigitale* by NGS were also identified as *T. interdigitale/mentagrophytes* or *T. mentagrophytes* Type IV using the DermaGenius® kits, and one strain was identified as *T. schoenleinii/quinckeanum* using both the DermaGenius® Resistance and 3.0 kits. All strains identified as *T. rubrum* by NGS were identified as *T. rubrum/soudanense* using the DermaGenius® kits. All strains identified as *T. mentagrophytes/benhamiae/europaeum/japonicum* or *A. benhamiae* by NGS were identified as *T. benhamiae* by DermaGenius®. All strains identified as *T. tonsurans* by NGS were also identified as *T. tonsurans* by DermaGenius®. All strains identified as *T. mentagrophytes/interdigitale/indotineae* or as *T. mentagrophytes/interdigitale/benhamiae/vanbreuseghemii* by NGS were identified as *T.*

interdigitale/mentagrophytes using DermaGenius[®]. Strains identified as *T. erinacei/benhamiae* by NGS were identified as *T. benhamiae* by DermaGenius[®].

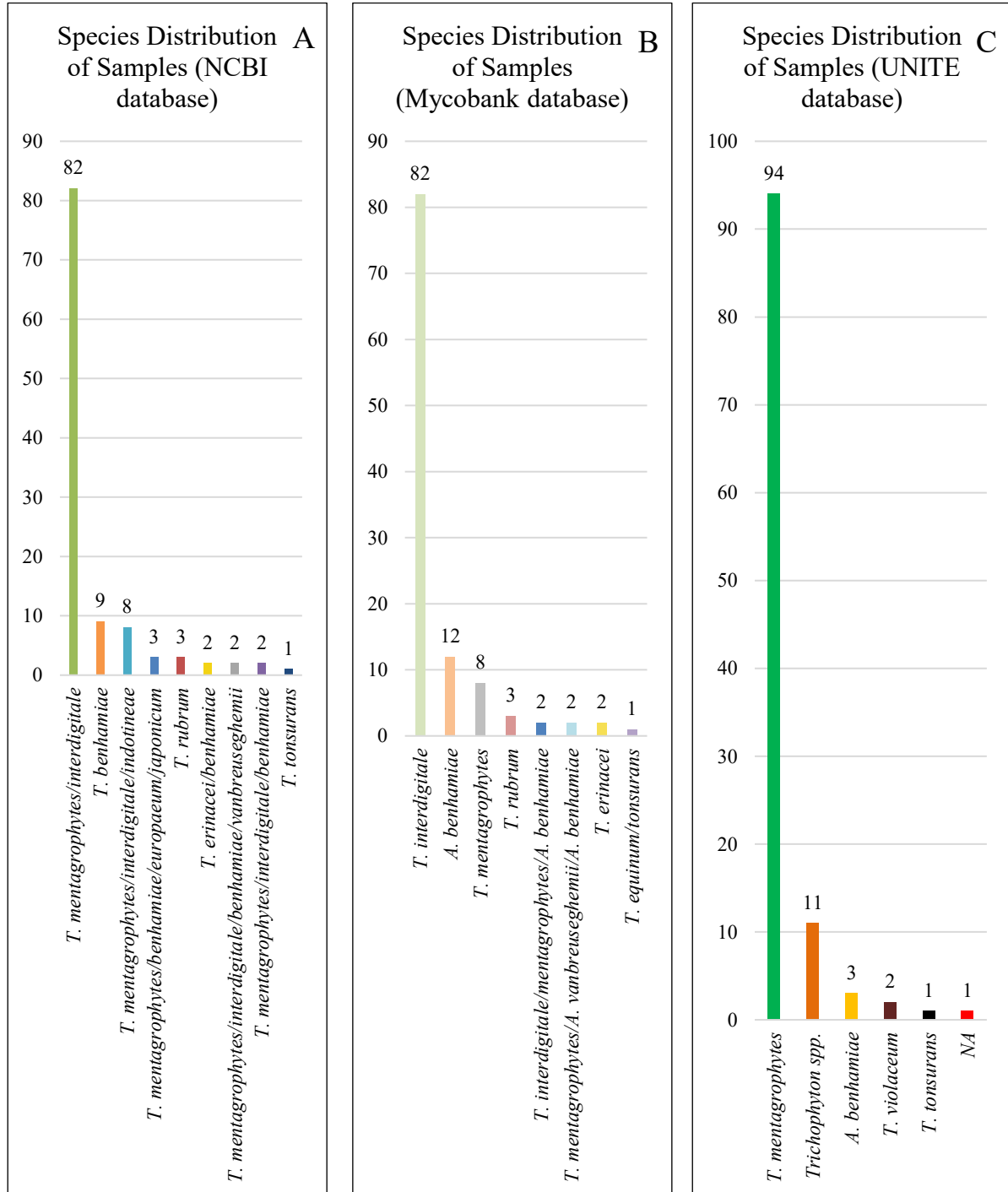


Figure 13: Species distribution of dermatophyte strains used in this study based on *ITS2* sequencing and consecutive BLAST using the NCBI (A), Mycobank (B) and UNITE (C) databases

As visible in Figure 14, NGS bioinformatics revealed five coding mutations in *ERG1* in strains identified as *T. mentagrophytes/interdigitale*. The two amino acid substitutions p.N352D (c.1054A>G) and p.S392A (c.1174T>G) were considered as (species-unspecific) *ERG1* polymorphisms, as they were present in *T. mentagrophytes/interdigitale* strains as well as other species featuring both normal and elevated MIC values.

The amino acid substitution p. L419F (c.1255C>T) was considered a species-specific *ERG1* polymorphism, as it was only present in strains with normal MIC values categorized as *T. mentagrophytes/interdigitale* or *T. mentagrophytes/interdigitale/benhamiae/vanbreuseghemii* by NGS and subsequent database comparison.

Finally, NGS analysis revealed the two substitutions p.L393S (c.1178T>C) and p.F397L (c.1189T>C), which were only present in terbinafine- and naftifine resistant strains. Furthermore, these strains were categorized as *T. mentagrophytes/interdigitale/indotineae*. The strain which featured the *ERG1* mutation p.L393S (c.1178T>C) was the NEQAS strain D301, which featured terbinafine and naftifine MIC values of 0.5 µg/mL and was determined as a *SQLE/ERG1* mutant using the PathoNostics DermaGenius® Resistance kit.

Two of the strains featuring a p.F397L (c.1189T>C) substitution were the strains 214677/16 and 216377/17 (*T. indotineae*) kindly provided by Labor Mölbis, which were shown to be treatment-resistant patient isolates featuring highly elevated terbinafine MIC values. (Nenoff et al. 2020) These isolates were also determined to feature *SQLE/ERG1* target (resistance) mutations according to the PathoNostics DermaGenius® Resistance kit.

The other two *T. indotineae* strains provided by Labor Mölbis (901538/18 and 205667/19) were also included in the NGS analysis. These strains did not return any resistance mutations in *ERG1* since even though these strains are classified as *T. indotineae*, they do not feature elevated terbinafine MIC values or treatment resistance to terbinafine. Moreover, Labor Mölbis did not report any terbinafine resistance mutations present in these strains. (Nenoff et al. 2020) However, these isolates were determined to contain the azole resistance mutation p.A448T in the *ERG1* gene by (Nenoff et al. 2020), though azole resistance is usually mediated via the *ERG11* gene (see 1.5.1). Nevertheless, we could not detect this mutation since the *ERG1* primers used in this study were located between 1049-1067 bp (forward primer) and 1424-1443

bp (reverse primer), resulting in an amplicon length of ≤ 394 bp. Since the amplified region contained an intron of 62 bp, the position p.A448 was not included.

The last strain with a p.F397L (c.1189T>C) mutation was the treatment-resistant patient isolate F1366 from the General Hospital of Vienna featuring a terbinafine MIC value of 4 $\mu\text{g/mL}$ and a naftifine MIC value of >8 $\mu\text{g/mL}$. This strain was also categorized as a *SQLE/ERG1* mutant by the PathoNostics DermaGenius[®] Resistance kit.

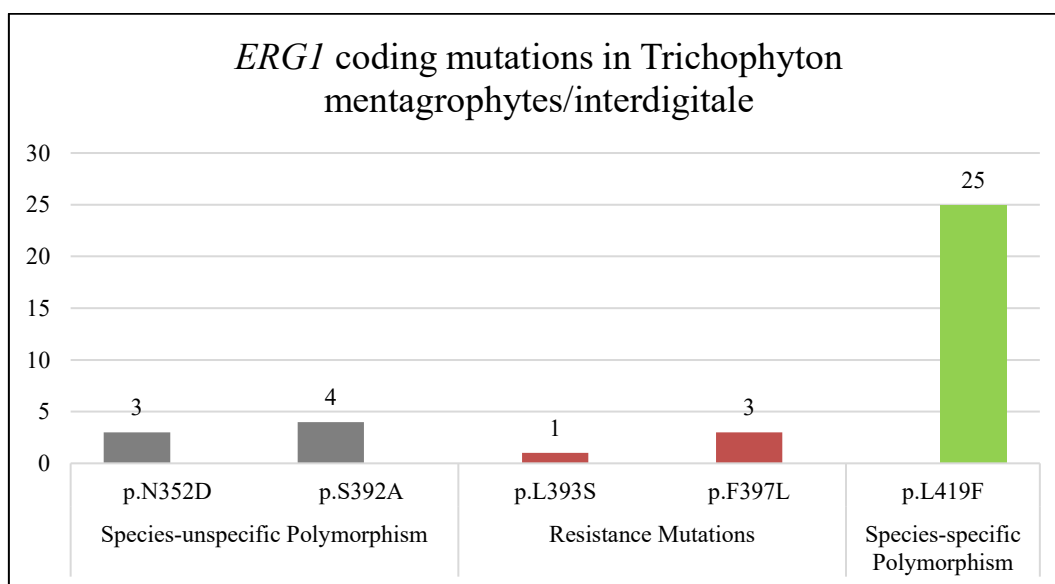


Figure 14: *ERG1* coding mutations and their corresponding amino acid substitutions in the squalene epoxidase protein in the *Trichophyton mentagrophytes/interdigitale* species complex

4 Discussion

4.1 *Trichophyton indotineae* and terbinafine resistance in Austria

One of the main objectives of this master thesis was to assess the spread of the *Trichophyton indotineae* to Austrian patients in retrospect. However, it is important to note that the sample volume was too small to generate a prevalence study, as only 52 strains were confirmed as clinical patient isolates. Furthermore, the timepoint of strain acquisition was only verified for 58 dermatophyte strains, and the number samples collected per year varied greatly, complicating the reasoning of the spread of this species in a time-dependent manner (see Figure 15). As the spread of resistant species in Europe, especially *T. indotineae*, is a relatively new

development, the prevalence of treatment-resistant dermatophytosis has only been measured recently and will likely continue to rise.

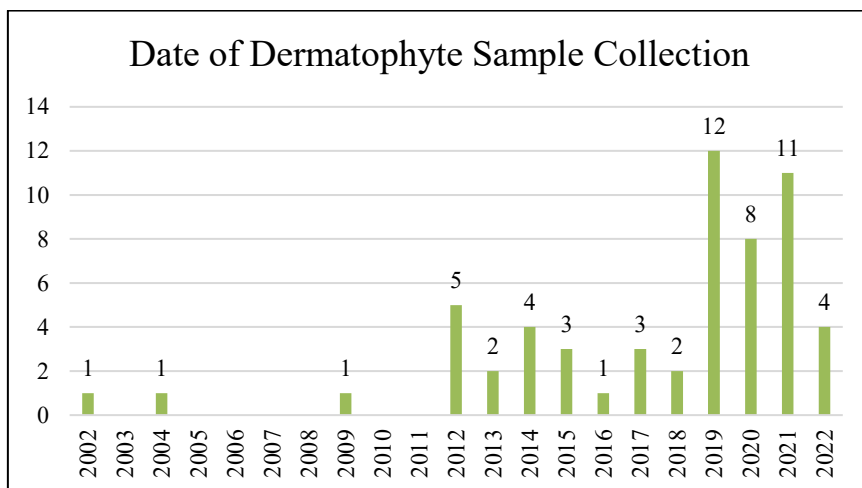


Figure 15: Date of the sample acquisition of the strains used in this study

However, it can be noted that within the 106 strains analysed in this study, three strains were identified as *T. mentagrophytes/interdigitale/indotinae* using NGS. These strains included the NEQAS strain D301, the treatment-resistant patient isolate F1366, and, most interestingly, the strain D187, which features average MIC values for all tested antifungals. Furthermore, five strains used for quality control purposes were also identified as *T. mentagrophytes/interdigitale/indotinae* by the NCBI BLAST. These strains consisted of four strains kindly provided by Labor Mölbis (214677/16, 216377/17, 901538/18, 205667/19) and one EUCAST strain (SSI-9363/CCUG 74948). As these quality control strains have already been verified as *T. indotinae* and since their ASV is identical to the two patient isolates F1366 and D187 as well as the NEQAS strain D301, it is likely that the three strains included in this study are also *T. indotinae* (*T. mentagrophytes*, ITS genotype VIII).

The NCBI-, Mycobank- and UNITE databases overall delivered dermatophyte species results with significant overlap. While the NCBI BLAST assigned a separate species identification to each different ASV (*ITS2* sequence), Mycobank seemed to provide slightly broader classifications grouping together genotypes deemed similar by both databases. The UNITE database sorted the strains into similar complexes as the other two databases, but specific species verification was unsuccessful in 11 out of 102 strains, and one strain could not be

identified. The UNITE database also identified all strains identified as *T. rubrum* by the other two databases as *T. violaceum*, including EUCAST quality control strains verified as *T. rubrum*. The distinction of closely related species or *ITS* genotypes within the *T. mentagrophytes/interdigitale* species complex was not possible using the UNITE database and only partly possible using the Mycobank database. As a result of this database comparison, only the NCBI database could distinct species within the *T. mentagrophytes/interdigitale* species complex to a level where five strains (214677/16, 216377/17, 901538/18, 205667/19, SSI-9363/CCUG 74948) verified as *T. indotineae* could be recognized as such. However, it is necessary to note that the UNITE database was made for mycobiome analysis. Due to the large amount of data necessary for general mycobiome analysis, the exact identification of closely related or rare fungal species is not within the scope of this database. However, considering the purpose of this database, the obtained results were surprisingly accurate.

While the NCBI BLAST seemed to offer more accurate results for *T. indotineae*, it is difficult to prove one of these databases as “always correct” or “always incorrect”. Dermatophyte species complexes are often very closely related, and species results may vary based on the database, complicating precise species identification. Furthermore, as the nomenclature of *T. mentagrophytes/interdigitale* strains has been changed recently (Nenoff et al. 2019a), some strains might be in the database under the old species name. In case a definite species classification is required, it might be necessary to either compare several databases or to cluster the strains in question to specific strains verified under the new nomenclature by hand using phylogenetic analysis. However, manual clustering using strains of a verified species is outright impractical when identifying a large number of strains.

(Tang et al. 2021) recently published a report identifying the HMG gene as a potential factor differentiating *T. indotineae* from other strains of the *T. mentagrophytes/interdigitale* species complex, thereby highlighting that a larger variety of genes might be available to better distinct dermatophyte species in the future.

4.2 Target Mutations in Terbinafine Resistance

This study found two terbinafine- and naftifine resistant strains featuring the *ERG1* target mutations c.1178T>C and c.1189T>C resulting in the amino acid substitutions p.L393S and p.F397L, respectively. All strains that showed elevated MIC values to terbinafine and naftifine featured one of these two mutations. Naftifine and terbinafine MIC values were always elevated in a concurrent manner, pointing to the possibility that these target mutations not only cause resistance to terbinafine, but that they may cause a cross-resistance to all allylamines – although further studies will need to be performed to confirm this hypothesis.

Interestingly, the *ERG1* target mutation p.S392 (c.1174T>G), which is only one amino acid apart from the hotspot region for resistance mutations did not seem to influence terbinafine or naftifine MIC values. Instead, it was identified as a non-causal *ERG1* variant/polymorphism (see 3.6). This phenomenon might be due to the interesting binding site of the terbinafine (and possibly also naftifine) molecule to the squalene epoxidase protein. (Saunte et al. 2019) modelled the drug-target binding site of terbinafine, superimposing the terbinafine molecule onto the *T. rubrum* squalene epoxidase protein using existing information from *Saccharomyces cerevisiae*. As visible in Figure 16, the terbinafine molecule binds into a groove in the 3D structure of the protein, only interacting with very specific residues instead of long stretches of the amino acid sequence. Thereby, this model explains the phenomenon observed in this study as well as the small number of mutations currently observed in terbinafine resistant strains.

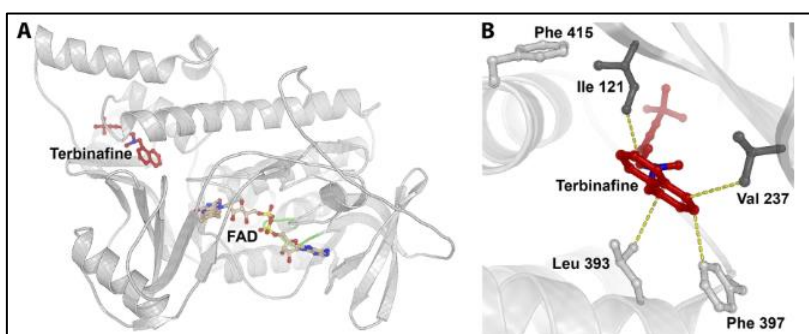


Figure 16: Model of the drug-target binding site of terbinafine to the squalene epoxidase protein (figure taken from (Saunte et al. 2019))

Finally, all strains featuring elevated terbinafine and naftifine MIC values and resistance mutations were identified as *T. indotinae*. Other strains of the *T. mentagrophytes/interdigitale* species complex did not feature potentially causal (resistance) mutations.

4.3 Target Mutations in Azole Resistance

While the MIC values for azoles observed in this study were rather high and arguably above EUCAST ECOFFs, no subpopulations with significantly elevated azole MIC values (compared to the population distribution) could be found in this study. Due to the lack of strains with significantly elevated azole MIC values, the *ERG11* gene was not sequenced. However, it can be noted that fluconazole on its own might not be the most effective antifungal against strains of the *T. mentagrophytes/interdigitale* species complex due to the high MIC values observed in all dermatophyte strains.

4.4 PathoNostics DermaGenius® Resistance/3.0 Multiplex real-time PCR

The *SQLE/ERG1* resistance detection by the PathoNostics DermaGenius® Resistance Multiplex real-time PCR kit in combination with the PathoNostics DermaGenius® 3.0 Complete Multiplex real-time PCR kit led to the same species results or similar species results as NGS for all 106 tested dermatophyte strains.

However, the DermaGenius® Resistance kit labelled four strains included in the experiment (F1330, D211, D301, D40) and one EUCAST quality control strain (SSI-9363/CCUG 74948) as *T. schoenleinii/quinckeanum*, while the DermaGenius® 3.0 kit labelled them as *T. interdigitale/mentagrophytes*. DADA2 analysis in combination with database search returned the species as *T. mentagrophytes/interdigitale* for three of these strains (F1330, D211, D40), while the other two (SSI-9363, D301) were categorized as *T. mentagrophytes/interdigitale/indotineae*.

Strains categorized as *T. benhamiae* using NGS or the DermaGenius® 3.0 kit could not be identified by using the Resistance kit (see 3.4), as they are not included as detectable species in this kit. Furthermore, other species which were not included in both kits were identified as another closely related species complex - *T. indotineae* was labelled as *T. interdigitale/mentagrophytes* or as *T. schoenleinii/quinckeanum* using both kits, and *T. erinacei/benhamiae* was not recognized using the DermaGenius® Resistance kit and labelled as *T. benhamiae* by the DermaGenius® 3.0 kit.

Overall, species identification using the DermaGenius® Resistance and 3.0 kits is a reliable means of roughly identifying dermatophyte species quickly and easily from patient material,

for instance in routine settings. However, the species identification provided by these kits is only accurate if the species in question is included in the kit, and species not included in the kit can be sorted into different species complexes without a warning by the program.

The DermaGenius[®] 3.0 kit generally offers a more reliable species identification (especially for less common dermatophytes) due the increased range of dermatophytes which can be detected. This study also found DermaGenius[®] 3.0 kit to be more accurate in identifying isolates of the *T. mentagrophytes/interdigitale* complex. Additionally, this kit offers a pan-dermatophyte PCR, which will return a positive result if dermatophyte DNA is detected (not tested in this study), which might greatly aid the routine determination of dermatophytosis otherwise confused with bacterial infections or other skin diseases. Therefore, the DermaGenius[®] 3.0 kit is more reliable than the Resistance kit in species identification, though if a definite species identification is needed, sequencing or microscopy of the isolates is still necessary.

The detection of the *ERG1* genotype using the DermaGenius[®] Resistance kit showed the same results as NGS in all 106 strains included in this study, plus reference strains. Even though the Resistance kit is only verified to detect the two most common target mutations p.L393F and p.F397L (Singh et al. 2021), we found that it was also able to detect the mutation p.L393S.

As the mutations p.L393F and p.F397L are present in the vast majority of resistant strains, it can be concluded that the DermaGenius[®] Resistance kit is a valid option for quickly and easily determining the most common resistance mutations in routine settings while only using patient material instead of pure culture material. However, it is necessary to note that other, less frequent resistance mutations in different loci might not be detected. Therefore, it is crucial to apply common sense when interpreting results from this kit. If a strain is reported as treatment-resistant but the DermaGenius[®] kit returns that the strain has no resistance mutations, it will still be necessary to perform antifungal susceptibility testing and/or NGS.

While the DermaGenius[®] Resistance kit is less reliable for the species identification of unknown dermatophyte strains, it offers the unparalleled benefit of detecting the most common *ERG1* terbinafine resistance mutations within mere hours of the arrival of patient material while still recognizing the most common dermatophytes in just one PCR. As the resistance status of dermatophytes isolated from a patient is usually more important for therapeutic interventions

than the exact species identification, the DermaGenius[®] Resistance kit might become an essential part of routine diagnostics for treatment-resistant dermatophytosis. Moreover, this kit could be supplemented by using the DermaGenius[®] 3.0 kit in case a more detailed species identification is wished. Therefore, the DermaGenius[®] Resistance kit may thereby greatly facilitate the diagnosis of terbinafine treatment-resistant strains and thereby improve treatment quality.

4.5 Conclusion and Outlook

This study has found three strains identified as *T. indotineae* within 106 sample strains in Austria. Two of these strains are patient isolates, and one is a NEQAS control strain. Two strains feature *ERG1* target mutations in combination with elevated allylamine MIC values (NEQAS control strain D301: TRB 0.5 µg/mL, NAF 0.5 µg/mL; *ERG1* mutation p.L393S) or highly elevated allylamine MIC values (patient isolate F1366: TRB 4 µg/mL, NAF >8 µg/mL; *ERG1* mutation p.F397L) and average azole MIC values. The third strain (patient isolate D187) featured average allylamine and azole MIC values. Itraconazole, miconazole, fluconazole, amorolfine, ciclopirox and griseofulvin MIC values feature a continuous distribution without outliers indicating resistant strains. Therefore, these antifungals might be alternative treatment options against all 106 strains observed in this thesis, including terbinafine- and naftifine resistant strains. However, as fluconazole MIC values appear rather high (1-256 µg/mL), fluconazole by itself might not be the best treatment option against strains of the *T. mentagrophytes/interdigitale* species complex, at least while other treatment options are still available.

The presence of *T. indotineae* strains with and without mutations in the *ERG1* resistance hotspots suggests that the dermatophyte species *T. indotineae* might not necessarily feature intrinsic antifungal resistance, as recently suggested by (Burmester et al. 2022). This theory is further supported by the resistance patterns observed in *T. indotineae* over the past few years. Several studies including, but not limited to (Yamada et al. 2017, Nenoff et al. 2020, Dellière et al. 2022) recently reported a large number of strains identified as *T. mentagrophytes* ITS genotype VIII (*T. indotineae*) featuring a variety of different target mutations conferring varying antifungal resistance patterns. While some strains featured terbinafine resistance, others were identified as resistant to certain azoles, and some did not show any resistance against either

of these antifungal classes. While the involvement of resistance mutations affecting several antifungal classes such as multidrug efflux pumps cannot be ruled out, the presence of varying, naturally occurring combinations of target mutations within the species *T. indotineae* indicates that antifungal resistance might not be an intrinsic feature of this species, but rather points to the possibility that these resistant strains belong to several subpopulations within the species classification of *T. indotineae*.

Even though the rate of elevated allylamine MIC levels and the number of isolates classified as *T. indotineae* are currently low, these results should not be taken lightly. As stated in 4.1, the sample volume and the percentage of (especially recent) clinical isolates used in this study was relatively low. Furthermore, antifungal resistance in dermatophytes has only recently been considered a threat due to the surge in cases of treatment-resistant dermatophytosis. As a result, many clinics and laboratories still do not assess the antifungal susceptibility or *ERG1* mutation status of treatment-resistant dermatophytes, leading to the persistence and potential spread of these resistant strains. As (Brasch et al. 2021) stated, the further dissemination of treatment-resistant strains of *T. indotineae* is “to be expected” due to their only mildly inflammatory nature among other factors. Furthermore, the treatment of dermatophytosis with corticosteroids with or without additional antifungal treatment is still an issue which should be seized after observing the situation in India. (Panda and Verma 2017, Nenoff et al. 2019b, Ebert et al. 2020, Verma et al. 2021c, 2022, Das et al. 2022)

However, even though the current situation seems grim, not all hope is lost. Collective attempts of adapting existing medications as well as developing new antifungals to combat resistant strains have been made by several research groups in several countries.

(Gawaz et al. 2021) recently published a case report after successfully treating a patient affected by a terbinafine-resistant strain classified as *T. indotineae* with adapted doses of super bioavailable itraconazole. The use of super bioavailable itraconazole in previously treatment-resistant cases is further supported by a study by (Sardana and Mathachan 2021).

(Sardana et al. 2021) further released a study containing a checkerboard analysis of existing antifungals used in dermatophytosis, highlighting potential synergistic effects of certain combinations against terbinafine- susceptible as well as -resistant isolates.

Furthermore, the novel antifungal olorofim, which targets an enzyme involved in *de novo* pyrimidine biosynthesis, shows promising preliminary results against a variety of mould isolates including dermatophytes. (Astvad et al. 2020)

To conclude, it would be wise to carefully consider how treatment resistance in dermatophytosis is currently handled in Austria. Antifungal susceptibility testing and – if necessary – *ERG1* mutation analysis using PCR kits or sequencing should be considered in treatment-resistant cases to reduce patient discomfort, treatment duration and the spread of resistant strains due to prolonged treatment times. Even though antifungal resistance is on the rise, terbinafine and azoles are still viable treatment options in most cases. Even in resistant cases, the use of different dosages or super bioavailable drug formulations as well as the use of antifungal combinations containing terbinafine and/or azoles (as mentioned above) might still be a valid option.

Abstract

Introduction and Aim

Dermatophytes are primary pathogenic, filamentous fungi infecting hair, skin and nails. Within the past six years, a novel terbinafine-resistant dermatophyte species termed *Trichophyton indotineae* (*Trichophyton mentagrophytes* ITS genotype VIII), which was first described in India, has spread to Europe, causing an “epidemic-like scenario” of treatment-resistant dermatophytosis. (Martinez-Rossi et al. 2018, Verma et al. 2021c) However, no studies on the prevalence of this species in Austria have been published so far. Therefore, this master thesis aims to assess the occurrence and potential terbinafine resistance mechanisms in strains identified as part of the *Trichophyton mentagrophytes/interdigitale* species complex in Austria.

Methods

106 dermatophyte strains identified as *Trichophyton mentagrophytes* (48 strains), *Trichophyton interdigitale* (48 strains), *Trichophyton indotineae* (1 strain), or of the *Trichophyton mentagrophytes/interdigitale* species complex (9 strains) were collected from laboratory test strains and from Austrian clinical isolates over the past 20 years. Antifungal susceptibility testing using the EUCAST microdilution method was performed for the antifungals amorolfine, miconazole, itraconazole, fluconazole, terbinafine, naftifine, griseofulvin and ciclopirox. *ERG1* target mutations that cause terbinafine- and possibly naftifine resistance were determined using the DermaGenius[®] Resistance Multiplex real-time PCR kit (Cat. No. PN-303, PathoNostics, Maastricht, Netherlands) and next-generation sequencing.

Results

All 106 strains featured low amorolfine, itraconazole, miconazole, fluconazole, griseofulvin, and ciclopirox MIC values. While 104 strains showed low terbinafine and naftifine MIC values, two strains had terbinafine/naftifine MIC values of 0.5/0.5 µg/mL and 4/>8 µg/mL, indicating resistance. The PathoNostics DermaGenius[®] Resistance Multiplex real-time PCR kit and next-generation sequencing confirmed the presence of *ERG1* target mutations.

Conclusion

Two isolates featured (highly) elevated MIC values to the two allylamines terbinafine and naftifine. As these strains also feature *ERG1* mutations, it is possible that they could be cross-resistant to allylamines based on an *ERG1* target mutation. Therefore, although the resistance rate is low, antifungal susceptibility testing should be considered in treatment-resistant cases.

Zusammenfassung

Einleitung und Ziel

Dermatophyten sind primär pathogene Fadenpilze, welche die Haut, Haare und Nägel infizieren. Innerhalb der letzten sechs Jahre hat sich die neuartige, terbinafinresistente Dermatophytenart *Trichophyton indotineae* (*Trichophyton mentagrophytes* ITS-Genotyp VIII), welche zuerst in Indien beschrieben wurde, bis nach Europa ausgebreitet und verursacht nun eine epidemieartige Welle an therapieresistenten Dermatomykosen. (Martinez-Rossi et al. 2018, Verma et al. 2021c) Da bisher noch keine Prävalenzstudien über resistente Dermatophyten in Österreich durchgeführt wurden, ist das Ziel dieser Masterarbeit, das Vorkommen sowie mögliche Resistenzmutationen im *Trichophyton mentagrophytes/interdigitale*-Spezieskomplex in Österreich festzustellen.

Methoden

106 Dermatophytenstämme, welche zuvor als *Trichophyton mentagrophytes* (48 Stämme), *Trichophyton interdigitale* (48 Stämme), *Trichophyton indotineae* (1 Stamm), oder als Teil des *Trichophyton mentagrophytes/interdigitale*-Spezieskomplex (9 Stämme) identifiziert wurden, wurden aus Labor-Teststämmen oder aus österreichischen Patientenisolaten innerhalb der letzten 20 Jahre gesammelt. Antimykotika-Resistenztestungen wurden mithilfe der EUCAST-Mikrodilutionsmethode für die Antimykotika Amorolfing, Miconazol, Itraconazol, Fluconazol, Terbinafin, Naftifin und Ciclopirox durchgeführt. *ERG1*-Targetmutationen, welche Terbinafin- und möglicherweise auch Naftifinresistenzen hervorrufen, wurden mithilfe des DermaGenius[®] Resistance Multiplex real-time PCR kit (Cat. No. PN-303, PathoNostics, Maastricht, Niederlande) und Next-Generation Sequencing ermittelt.

Resultate

Alle 106 Dermatophytenstämme wiesen niedrige Amorolfin-, Itraconazol-, Miconazol-, Fluconazol-, Griseofulvin-, und Ciclopirox-MHK-Werte auf. 104 Stämme hatten niedrige Terbinafin- und Naftifin-MHK-Werte, während zwei Stämme erhöhte Terbinafin-/Naftifin-MHK-Werte von 0.5/0.5 µg/mL und 4/>8 µg/mL hatten, welche für eine Resistenz sprechen könnten. Die Präsenz von *ERG1*-Targetmutationen wurde mithilfe vom PathoNostics

DermaGenius[®] Resistance Multiplex real-time PCR kit und von Next-Generation Sequencing nachgewiesen.

Konklusion

Zwei Isolate, welche (stark) erhöhte MHK-Werte gegen die Allylamine Terbinafin und Naftifin aufwiesen, weisen *ERGI*-Targetmutationen auf. Da erhöhte Terbinafin- und Naftifin-MHK-Werte stets gemeinsam auftreten, besteht die Möglichkeit, dass *ERGI*-Targetmutationen Kreuzresistenzen gegen alle Antimykotika der Klasse der Allylamine hervorrufen. Daher sollte die Antimykotika-Resistenztestung in behandlungsresistenten Fällen trotz der niedrigen Resistenzrate in dieser Studie in Erwägung gezogen werden.

List of Abbreviations

<i>A.</i>	<i>Arthroderma</i>
ABC	ATP Binding Cassette (transporter superfamily)
AMR	Amorolfine (hydrochloride)
CLSI	Clinical & Laboratory Standards Institute
CPX	Ciclopirox (olamine)
<i>E.</i>	<i>Epidermopyton</i>
ECOFF	Epidemiological cut-off
EUCAST	European Committee on Antimicrobial Susceptibility Testing
FLC	Fluconazole
GRS	Griseofulvin
HSP	heat shock protein
ITC	Itraconazole
<i>M.</i>	<i>Microsporum</i>
MCZ	Miconazole
MIC	minimum inhibitory concentration
MFC	minimum fungicidal concentration
MFS	major facilitator superfamily
MDR	multidrug resistance
NAF	Naftifine
NGS	Next-Generation Sequencing
<i>S.</i>	<i>Saccharomyces</i>
SC	stratum corneum
SNP	single nucleotide polymorphism
SQLE/SE	squalene epoxidase
TRB	terbinafine
<i>T.</i>	<i>Trichophyton</i>

List of Figures

Figure 1: Aims of this master thesis (created with BioRender.com)	8
Figure 2: Species distribution of the dermatophyte culture collection of the Department of Clinical Microbiology, General Hospital of Vienna	24
Figure 3: Layout of dermatophyte microdilution plates	26
Figure 4: Illumina plate layout featuring the index primer combinations	37
Figure 5: Macroscopic culture morphology of strains confirmed as part of the <i>T. mentagrophytes/interdigitale</i> species complex using NGS (see 3.6)	40
Figure 6: Lactophenol blue staining of strains confirmed as part of the <i>T. mentagrophytes/interdigitale</i> species complex, 40x and 100x magnification (light microscopy); purple arrows: microconidia, yellow arrows: macroconidia, green arrows: spiral hyphae, red arrows: spherical structures	41
Figure 7: Minimum inhibitory concentration distributions of commonly used antifungals against strains of the <i>T. mentagrophytes/interdigitale</i> species complex; ECOFF values are taken from (European Committee on Antimicrobial Susceptibility Testing 2022) for <i>Trichophyton indotineae</i>	44
Figure 8: Dermatophyte growth before (left) and during/after (right) induction of <i>in vitro</i> resistance; changes in growth pattern applicable for all strains (n=5)	45
Figure 9: Species identification of dermatophyte strains using melting curve analysis (PathoNostics® DermaGenius® Resistance Multiplex real-time PCR kit)	46
Figure 10: Results of the test run of the specific <i>ERG1/ITS2</i> PCR	49
Figure 11: Results of the specific <i>ERG1/ITS2</i> PCR, main run; A: First run, plate 1; B: First run, plate 2 + second loading of samples without bands; C: Second run; repetition PCR of unsuccessfully amplified samples	50
Figure 12: NGS run parameters; A: run summary, B: thumbnail of amplified clusters; C: quality scores; D: heatmap of quality scores throughout the run	51
Figure 13: Species distribution of dermatophyte strains used in this study based on <i>ITS2</i> sequencing and consecutive BLAST using the NCBI (A), Mycobank (B) and UNITE (C) databases	53

Figure 14: <i>ERG1</i> coding mutations and their corresponding amino acid substitutions in the squalene epoxidase protein in the <i>Trichophyton mentagrophytes/interdigitale</i> species complex	55
Figure 15: Date of the sample acquisition of the strains used in this study	56
Figure 16: Model of the drug-target binding site of terbinafine to the squalene epoxidase protein (figure taken from (Saunte et al. 2019))	58

List of Tables

Table 1: <i>ITS</i> genotypes and geographic origins of the <i>T. mentagrophytes/interdigitale</i> complex; data taken from (Verma et al. 2021b)	12
Table 2: Reference MICs used to analyse the dermatophyte MIC level observed in this study; []: Values in square brackets are tentative ECOFFs set by the EUCAST; ¹ : Source: (European Committee on Antimicrobial Susceptibility Testing 2022); *: Determined using the CLSI broth microdilution method	25
Table 3: Components of the DermaGenius [®] PCR reaction	32
Table 4: DermaGenius [®] PCR protocol	32
Table 5: Primers and Illumina overhang adapters for the specific PCR of dermatophytes	34
Table 6: PCR components for the dermatophyte PCR	35
Table 7: PCR programs for the <i>ERG1/ITS2</i> and the Illumina index PCR	36
Table 8: Species identification of clinical dermatophyte isolates using the PathoNostics DermaGenius [®] Resistance Multiplex real-time PCR kit	47
Table 9: Species identification of clinical dermatophyte isolates using the PathoNostics DermaGenius [®] 3.0 Complete Multiplex real-time PCR kit	47
Table 10: SQLE/ <i>ERG1</i> genotype identification of clinical dermatophyte isolates using the PathoNostics DermaGenius [®] Resistance Multiplex real-time PCR kit	48

References

- de Aguiar Peres NT, Maranhão FCA, Rossi A, Martinez-Rossi NM. 2010. Dermatophytes: Host-pathogen interaction and antifungal resistance. *Anais Brasileiros de Dermatologia*, 85(5):657–667.
- Arendrup MC, Kahlmeter G, Guinea J, Meletiadis J. 2021. How to: perform antifungal susceptibility testing of microconidia-forming dermatophytes following the new reference EUCAST method E.Def 11.0, exemplified by *Trichophyton*. *Clinical Microbiology and Infection*, 27(1):55–60.
- Arrese J, Piérard-Franchimont C, Piérard G. 2001. A plea to bridge the gap between antifungals and the management of onychomycosis. *American journal of clinical dermatology*, 2(5):281–284.
- Astvad KMT, Jørgensen KM, Hare RK, Datcu R, Arendrup MC. 2020. Olorofim Susceptibility Testing of 1,423 Danish Mold Isolates Obtained in 2018-2019 Confirms Uniform and Broad-Spectrum Activity. *Antimicrobial agents and chemotherapy*, 65(1).
- Astvad KMT, Hare RK, Jørgensen KM, Saunte DML, Thomsen PK, Arendrup MC. 2022. Increasing Terbinafine Resistance in Danish *Trichophyton* Isolates 2019-2020. *Journal of Fungi* 2022, Vol. 8, Page 150, 8(2):150.
- Baghi N, Shokohi T, Badalie H, Makimura K, Rezaei-Matehkolaei A, Abdollahi M, Didehdar M, Haghani I, Abastabar M. 2016. In vitro activity of new azoles luliconazole and lanconazole compared with ten other antifungal drugs against clinical dermatophyte isolates. *Medical mycology*, 54(7):757–763.
- Baldo A, Monod M, Mathy A, Cambier L, Bagut ET, Defaweux V, Symoens F, Antoine N, Mignon B. 2012. Mechanisms of skin adherence and invasion by dermatophytes. *Mycoses*, 55(3):218–223.
- Barker KS, Crisp S, Wiederhold N, Lewis RE, Bareither B, Eckstein J, Barbuch R, Bard M, Rogers PD. 2004. Genome-wide expression profiling reveals genes associated with amphotericin B and fluconazole resistance in experimentally induced antifungal resistant isolates of *Candida albicans*. *Journal of Antimicrobial Chemotherapy*, 54(2):376–385.

- Bitencourt TA, Lang EAS, Sanches PR, Peres NTA, Oliveira VM, Fachin AL, Rossi A, Martinez-Rossi NM. 2020. *HacA* Governs Virulence Traits and Adaptive Stress Responses in *Trichophyton rubrum*. *Frontiers in Microbiology*, 0:193.
- Borghesi E, Borgo F, Morace G. 2016. Fungal biofilms: Update on resistance. *Advances in Experimental Medicine and Biology*, 931.
- Brasch J, Gräser Y, Beck-Jendroscheck V, Voss K, Torz K, Walther G, Schwarz T. 2021. “Indian” strains of *Trichophyton mentagrophytes* with reduced itraconazole susceptibility in Germany. *JDDG - Journal of the German Society of Dermatology*, 19(12):1723–1727.
- Brilhante R, Correia E, Guedes G, de Oliveira J, Castelo-Branco D, Cordeiro R, Pinheiro A, Chaves L, Pereira Neto W, Sidrim J, et al. 2018. In vitro activity of azole derivatives and griseofulvin against planktonic and biofilm growth of clinical isolates of dermatophytes. *Mycoses*, 61(7):449–454.
- Brilhante R, Aguiar L, Sales J, Araújo G, Pereira V, Pereira-Neto W, Pinheiro A, Paixão G, Cordeiro R, Sidrim J, et al. 2019. Ex vivo biofilm-forming ability of dermatophytes using dog and cat hair: an ethically viable approach for an infection model. *Biofouling*, 35(4):392–400.
- Burkhardt CN, Burkhardt CG, Gupta AK. 2002. Dermatophytoma: Recalcitrance to treatment because of existence of fungal biofilm. *Journal of the American Academy of Dermatology*, 47(4):629–631.
- Burmester A, Hipler UC, Hensche R, Elsner P, Wiegand C. 2019. Point mutations in the squalene epoxidase gene of Indian ITS genotype VIII *T. mentagrophytes* identified after DNA isolation from infected scales. *Medical Mycology Case Reports*, 26:23–24.
- Burmester A, Hipler UC, Uhrlaß S, Nenoff P, Singal A, Verma SB, Elsner P, Wiegand C. 2020. Indian *Trichophyton mentagrophytes* squalene epoxidase *erg1* double mutants show high proportion of combined fluconazole and terbinafine resistance. *Mycoses*, 63(11):1175–1180.

- Burmester A, Hipler UC, Elsner P, Wiegand C. 2022. Point mutations in the squalene epoxidase *erg1* and sterol 14- α demethylase *erg11* gene of *T. indotineae* isolates indicate that the resistant mutant strains evolved independently. *Mycoses*, 65(1):97–102.
- Campbell CK, Johnson EM, Warnock DW. 2013. *Moulds with Aleuriomycetes: I. The Dermatophytes. Identification of Pathogenic Fungi*. 31–79, John Wiley & Sons, Ltd;
- Campoy S, Adrio JL. 2017. Antifungals. *Biochemical Pharmacology*, 133:86–96.
- Castelo-Branco D, Aguiar L, Araújo G, Lopes R, Sales J, Pereira-Neto W, Pinheiro A, Paixão G, Cordeiro R, Sidrim J, et al. 2020. In vitro and ex vivo biofilms of dermatophytes: a new panorama for the study of antifungal drugs. *Biofouling*, 36(7):783–791.
- Cauwenbergh G, Degreef H, Heykants J, Woestenborghs R, van Rooy P, Haeverans K. 1988. Pharmacokinetic profile of orally administered itraconazole in human skin. *Journal of the American Academy of Dermatology*, 18(2):263–268.
- Cervellati EP, Fachin AL, Ferreira-Nozawa MS, Martinez-Rossi NM. 2006. Molecular cloning and characterization of a novel ABC transporter gene in the human pathogen *Trichophyton rubrum*. *Medical Mycology*, 44(2):141–147.
- Costa-Orlandi CB, Sardi JCO, Santos CT, Fusco-Almeida AM, Mendes M. 2014. In vitro characterization of *Trichophyton rubrum* and *T. mentagrophytes* biofilms. *Biofouling*, 30(6):719–727.
- Cowen LE, Sanglard D, Howard SJ, Rogers PD, Perlin DS. 2015. Mechanisms of antifungal drug resistance. *Cold Spring Harbor Perspectives in Medicine*, 5(7).
- Das A, Sil A, Verma SB, Kumar S. 2022. *Tinea pseudoimbricata*: observations from a clinicoepidemiological and mycological study from eastern India. *Clinical and Experimental Dermatology*, 47(1):147–149.
- Dellière S, Joannard B, Benderdouche M, Mingui A, Gits-Muselli M, Hamane S, Alanio A, Petit A, Gabison G, Bagot M, et al. 2022. Emergence of Difficult-to-Treat *Tinea Corporis* Caused by *Trichophyton mentagrophytes* Complex Isolates, Paris, France. *Emerging infectious diseases*, 28(1):224–228.

- Diao Y, Zhao R, Deng X, Leng W, Peng J, Jin Q. 2009. Transcriptional profiles of *Trichophyton rubrum* in response to itraconazole. *Medical Mycology*, 47(3):237–247.
- Dunkel N, Liu TT, Barker KS, Homayouni R, Morschhäuser J, Rogers PD. 2008. A gain-of-function mutation in the transcription factor Upc2p causes upregulation of ergosterol biosynthesis genes and increased fluconazole resistance in a clinical *Candida albicans* isolate. *Eukaryotic Cell*, 7(7):1180–1190.
- Ebert A, Monod M, Salamin K, Burmester A, Uhrlaß S, Wiegand C, Hipler UC, Krüger C, Koch D, Wittig F, et al. 2020. Alarming India-wide phenomenon of antifungal resistance in dermatophytes: A multicentre study. *Mycoses*, 63(7):717–728.
- European Committee on Antimicrobial Susceptibility Testing. 2022. Overview of antifungal ECOFFs and clinical breakpoints for yeasts, moulds and dermatophytes using the EUCAST E.Def 7.3, E.Def 9.4 and E.Def 11.0 procedures. Version 3.
- Fachin AL, Ferreira-Nozawa MS, Maccheroni W, Martinez-Rossi NM. 2006. Role of the ABC transporter TruMDR2 in terbinafine, 4-nitroquinoline N-oxide and ethidium bromide susceptibility in *Trichophyton rubrum*. *Journal of Medical Microbiology*, 55(8):1093–1099.
- Faergemann J, Zehender H, Millerioux L. 1994. Levels of terbinafine in plasma, stratum corneum, dermis–epidermis (without stratum corneum), sebum, hair and nails during and after 250 mg terbinafine orally once daily for 7 and 14 days. *Clinical and Experimental Dermatology*, 19(2):121–126.
- Faway É, Lambert de Rouvroit C, Poumay Y. 2018. In vitro models of dermatophyte infection to investigate epidermal barrier alterations. *Experimental dermatology*, 27(8):915–922.
- Ferreira-Nozawa MS, Silveira HCS, Ono CJ, Fachin AL, Rossi A, Martinez-Rossi NM. 2006. The pH signaling transcription factor PacC mediates the growth of *Trichophyton rubrum* on human nail in vitro. *Medical Mycology*, 44(7):641–645.
- Galdiero E, de Alteriis E, de Natale A, D’Alterio A, Siciliano A, Guida M, Lombardi L, Falanga A, Galdiero S. 2020. Eradication of *Candida albicans* persister cell biofilm by the membranotropic peptide gH625. *Scientific Reports* 2020 10:1, 10(1):1–12.

- Gaurav V, Bhattacharya SN, Sharma N, Datt S, Kumar P, Rai G, Singh PK, Taneja B, Das S. 2021. Terbinafine resistance in dermatophytes: Time to revisit alternate antifungal therapy. *Journal de Mycologie Medicale*, 31(1).
- Gawaz A, Nenoff P, Uhrlaß S, Schaller M. 2021. Treatment of a terbinafine-resistant trichophyton mentagrophytes type VIII. *Hautarzt*, 72(10):900–904.
- Ghannoum M. 2016. Azole resistance in dermatophytes: Prevalence and mechanism of action. *Journal of the American Podiatric Medical Association*, 106(1):79–86.
- Ghannoum M, Isham N, Verma A, Plaum S, Fleischer A, Jr., Hardas B. 2013. In Vitro Antifungal Activity of Naftifine Hydrochloride against Dermatophytes. *Antimicrobial Agents and Chemotherapy*, 57(9):4369.
- Gnat S, Łagowski D, Nowakiewicz A, Osińska M, Kopiński Ł. 2020. Population differentiation, antifungal susceptibility, and host range of *Trichophyton mentagrophytes* isolates causing recalcitrant infections in humans and animals. *European Journal of Clinical Microbiology and Infectious Diseases*, 39(11):2099–2113.
- Graminha MAS, Rocha EMF, Prade RA, Martinez-Rossi NM. 2004. Terbinafine resistance mediated by salicylate 1-monooxygenase in *Aspergillus nidulans*. *Antimicrobial Agents and Chemotherapy*, 48(9):3530–3535.
- Guarro J, Gené J, Stchigel AM. 1999. Developments in fungal taxonomy. *Clinical Microbiology Reviews*, 12(3):454–500.
- Gupta AK, Kohli Y. 2003. In vitro susceptibility testing of ciclopirox, terbinafine, ketoconazole and itraconazole against dermatophytes and nondermatophytes, and in vitro evaluation of combination antifungal activity. *British Journal of Dermatology*, 149(2):296–305.
- Gupta AK, Renaud HJ, Quinlan EM, Shear NH, Piguet V. 2021. The Growing Problem of Antifungal Resistance in Onychomycosis and Other Superficial Mycoses. *American Journal of Clinical Dermatology*, 22(2):149–157.
- Havlickova B, Czaika VA, Friedrich M. 2008. Epidemiological trends in skin mycoses worldwide. *Mycoses*, 51 Suppl 4(SUPPL.4):2–15.

- Hazen KC. 1998. Fungicidal versus fungistatic activity of terbinafine and itraconazole: An in vitro comparison. *Journal of the American Academy of Dermatology*, 38(5 III).
- Hazen KC. 2000. Evaluation of in vitro susceptibility of dermatophytes to oral antifungal agents. *Journal of the American Academy of Dermatology*, 43(5):S125–S129.
- Hofbauer B, Leitner I, Ryder NS. 2002. In vitro susceptibility of *Microsporum canis* and other dermatophyte isolates from veterinary infections during therapy with terbinafine or griseofulvin. *Medical Mycology*, 40(2):179–183.
- de Hoog GS, Dukik K, Monod M, Packeu A, Stubbe D, Hendrickx M, Kupsch C, Stielow JB, Freeke J, Göker M, et al. 2017. Toward a Novel Multilocus Phylogenetic Taxonomy for the Dermatophytes. *Mycopathologia*, 182(1):5.
- Hsieh A, Quenan S, Riat A, Toutous-Trellu L, Fontao L. 2019. A new mutation in the SQLE gene of *Trichophyton mentagrophytes* associated to terbinafine resistance in a couple with disseminated tinea corporis. *Journal de Mycologie Medicale*, 29(4):352–355.
- Jacob TR, Peres NTA, Martins MP, Lang EAS, Sanches PR, Rossi A, Martinez-Rossi NM. 2015. Heat shock protein 90 (Hsp90) as a molecular target for the development of novel drugs against the dermatophyte *Trichophyton rubrum*. *Frontiers in Microbiology*, 6(NOV):1241.
- Järv H, Uhrlass S, Simkin T, Nenoff P, Alvarado Ramirez E, Chryssanthou E, Monod M. 2019. Terbinafine resistant *Trichophyton mentagrophytes* genotype VIII, Indian type, isolated in Finland. 9th Trends in Medical Mycology Held on 11–14 October 2019, Nice, France, Organized under the Auspices of EORTC-IDG and ECMM. 117–118, *Journal of Fungi*;
- Jiang Y, Luo W, Verweij PE, Song Y, Zhang B, Shang Z, Al-Hatmi AMS, Ahmed SA, Wan Z, Li R, et al. 2021. Regional Differences in Antifungal Susceptibility of the Prevalent Dermatophyte *Trichophyton rubrum*. *Mycopathologia*, 186(1):53–70.
- Kakurai M, Harada K, Maeda T, Hiruma J, Kano R, Demitsu T. 2020. Case of tinea corporis due to terbinafine-resistant *Trichophyton interdigitale*. *Journal of Dermatology*, 47(4):e104–e105.

- Kano R, Hsiao YH, Han HS, Chen C, Hasegawa A, Kamata H. 2018. Resistance Mechanism in a Terbinafine-Resistant Strain of *Microsporium canis*. *Mycopathologia*, 183(3):623–627.
- Kano R, Kimura U, Kakurai M, Hiruma J, Kamata H, Suga Y, Harada K. 2020. *Trichophyton indotineae* sp. nov.: A New Highly Terbinafine-Resistant Anthropophilic Dermatophyte Species. *Mycopathologia*, 185(6):947–958.
- Kano R, Noguchi H, Harada K, Hiruma M. 2021. Rapid Molecular Detection of Terbinafine-resistant Dermatophytes. *Medical mycology journal*, 62(2):41–44.
- Khurana A, Masih A, Chowdhary A, Sardana K, Borker S, Gupta A, Gautam RK, Sharma PK, Jain D. 2018. Correlation of in vitro susceptibility based on MICs and squalene epoxidase mutations with clinical response to terbinafine in patients with *Tinea corporis/cruris*. *Antimicrobial Agents and Chemotherapy*, 62(12).
- Khurana A, Sardana K, Chowdhary A. 2019. Antifungal resistance in dermatophytes: Recent trends and therapeutic implications. *Fungal Genetics and Biology*, 132.
- Kimura U, Hiruma M, Kano R, Matsumoto T, Noguchi H, Takamori K, Suga Y. 2020. Caution and warning: Arrival of terbinafine-resistant *Trichophyton interdigitale* of the Indian genotype, isolated from extensive dermatophytosis, in Japan. *Journal of Dermatology*, 47(5):e192–e193.
- Klinger M, Theiler M, Bosshard PP. 2021. Epidemiological and clinical aspects of *Trichophyton mentagrophytes*/*Trichophyton interdigitale* infections in the Zurich area: a retrospective study using genotyping. *Journal of the European Academy of Dermatology and Venereology*, 35(4):1017–1025.
- Kong X, Tang C, Singh A, Ahmed SA, Al-Hatmi AMS, Chowdhary A, Nenoff P, Gräser Y, Hainsworth S, Zhan P, et al. 2021. Antifungal susceptibility and mutations in the squalene epoxidase gene in dermatophytes of the *Trichophyton mentagrophytes* species complex. *Antimicrobial Agents and Chemotherapy*.

- LeBlanc E v., Polvi EJ, Veri AO, Privé GG, Cowen LE. 2020. Structure-guided approaches to targeting stress responses in human fungal pathogens. *The Journal of Biological Chemistry*, 295(42):14458.
- Manzano-Gayosso P, Méndez-Tovar LJ, Hernández-Hernández F, López-Martínez R. 2007. [Antifungal resistance: an emerging problem in Mexico]. *Gaceta medica de Mexico*, 144(1):23–6.
- Maranhão FCA, Paião FG, Martinez-Rossi NM. 2007. Isolation of transcripts over-expressed in human pathogen *Trichophyton rubrum* during growth in keratin. *Microbial Pathogenesis*, 43(4):166–172.
- Maranhão FCA, Paião FG, Fachin AL, Martinez-Rossi NM. 2009. Membrane transporter proteins are involved in *Trichophyton rubrum* pathogenesis. *Journal of Medical Microbiology*, 58(2):163–168.
- Marques De Araujo E, le Pape P, Gonçalves De Lima-Neto R, Gonçalves T, Buarque De Gusmao N. 2019. Induction of antifungal resistance exerted by the exposure of paclitaxel to *Aspergillus fumigatus* - *Aspergillus* and *Aspergillosis*.
- Martinez-Rossi NM, Peres NTA, Rossi A. 2008. Antifungal resistance mechanisms in dermatophytes. *Mycopathologia*, 166(5–6):369–383.
- Martinez-Rossi NM, Jacob TR, Sanches PR, Peres NTA, Lang EAS, Martins MP, Rossi A. 2016. Heat Shock Proteins in Dermatophytes: Current Advances and Perspectives. *Current Genomics*, 17(2):99–111.
- Martinez-Rossi NM, Bitencourt TA, Peres NTA, Lang EAS, Gomes E v., Quaresimin NR, Martins MP, Lopes L, Rossi A. 2018. Dermatophyte resistance to antifungal drugs: Mechanisms and prospectus. *Frontiers in Microbiology*, 9(MAY).
- Martins MP, Franceschini ACC, Jacob TR, Rossi A, Martinez-Rossi NM. 2016. Compensatory expression of multidrug-resistance genes encoding ABC transporters in dermatophytes. *Journal of Medical Microbiology*, 65(7):605–610.

- Monod M, Méhul B. 2019. Recent findings in onychomycosis and their application for appropriate treatment. *Journal of Fungi*, 5(1).
- Monod M, Feuermann M, Salamin K, Fratti M, Makino M, Alshahni MM, Makimura K, Yamada T. 2019. *Trichophyton rubrum* azole resistance mediated by a new ABC transporter, TruMDR3. *Antimicrobial Agents and Chemotherapy*, 63(11).
- Mota CRA, Miranda KC, Lemos JDA, Costa CR, Hasimoto E Souza LK, Passos XS, Meneses E Silva H, Silva MDRR. 2009. Comparison of in vitro activity of five antifungal agents against dermatophytes, using the agar dilution and broth microdilution methods. *Revista da Sociedade Brasileira de Medicina Tropical*, 42(3):250–254.
- Mukherjee PK, Leidich SD, Isham N, Leitner I, Ryder NS, Ghannoum MA. 2003. Clinical *Trichophyton rubrum* strain exhibiting primary resistance to terbinafine. *Antimicrobial Agents and Chemotherapy*, 47(1):82–86.
- Nenoff P, Verma SB, Uhrlaß S, Burmester A, Gräser Y. 2019a. A clarion call for preventing taxonomical errors of dermatophytes using the example of the novel *Trichophyton mentagrophytes* genotype VIII uniformly isolated in the Indian epidemic of superficial dermatophytosis. *Mycoses*, 62(1):6–10.
- Nenoff P, Verma SB, Vasani R, Burmester A, Hipler UC, Wittig F, Krüger C, Nenoff K, Wiegand C, Saraswat A, et al. 2019b. The current Indian epidemic of superficial dermatophytosis due to *Trichophyton mentagrophytes*—A molecular study. *Mycoses*, 62(4).
- Nenoff P, Verma SB, Ebert A, Süß A, Fischer E, Auerswald E, Dessoï S, Hofmann W, Schmidt S, Neubert K, et al. 2020. Spread of terbinafine-resistant *trichophyton mentagrophytes* type VIII (India) in Germany—“the tip of the iceberg?” *Journal of Fungi*, 6(4):1–20.
- Neyfakh AA. 2002. Mystery of multidrug transporters: The answer can be simple. *Molecular Microbiology*, 44(5):1123–1130.
- Nizam TM, Binting RAAG, Saari SM, Kumar TV, Muhammad M, Satim H, Yusoff H, Santhanam J. 2016. In Vitro Antifungal Activities against Moulds Isolated from

- Dermatological Specimens. *The Malaysian Journal of Medical Sciences : MJMS*, 23(3):32.
- Noguchi H, Matsumoto T, Hiruma M, Kimura U, Kashiwada-Nakamura K, Kubo M, Yaguchi T, Fukushima S, Kano R. 2021. Cluster infection caused by a terbinafine-resistant dermatophyte at a group home: The first case series in Japan. *Acta Dermatovenereologica*, 101(9).
- Osborne CS, Hofbauer B, Favre B, Ryder NS. 2003. In Vitro Analysis of the Ability of *Trichophyton rubrum* To Become Resistant to Terbinafine. *Antimicrobial Agents and Chemotherapy*, 47(11):3634–3636.
- Osborne CS, Leitner I, Favre B, Ryder NS. 2004. Antifungal drug response in an in vitro model of dermatophyte nail infection. *Medical Mycology*, 42(2):159–163.
- Osborne CS, Leitner I, Favre B, Ryder NS. 2005. Amino acid substitution in *Trichophyton rubrum* squalene epoxidase associated with resistance to terbinafine. *Antimicrobial Agents and Chemotherapy*, 49(7):2840–2844.
- Osborne CS, Leitner I, Hofbauer B, Fielding CA, Favre B, Ryder NS. 2006. Biological, biochemical, and molecular characterization of a new clinical *Trichophyton rubrum* isolate resistant to terbinafine. *Antimicrobial Agents and Chemotherapy*, 50(6):2234–2236.
- Pai V, Ganavalli A, Kikkeri NN. 2018. Antifungal resistance in dermatology. *Indian Journal of Dermatology*, 63(5):361–368.
- Paião FG, Segato F, Cursino-Santos JR, Peres NTA, Martinez-Rossi NM. 2007. Analysis of *Trichophyton rubrum* gene expression in response to cytotoxic drugs. *FEMS Microbiology Letters*, 271(2):180–186.
- Panda S, Verma S. 2017. The menace of dermatophytosis in India: The evidence that we need. *Indian Journal of Dermatology, Venereology and Leprology*, 83(3):281–284.
- Pashootan N, Shams-Ghahfarokhi M, Chaichi Nusrati A, Salehi Z, Asmar M, Razzaghi-Abyaneh M. 2022. Phylogeny, Antifungal Susceptibility, and Point Mutations of SQLE

- Gene in Major Pathogenic Dermatophytes Isolated From Clinical Dermatophytosis. *Frontiers in Cellular and Infection Microbiology*, 12:217.
- Pasrija R, Krishnamurthy S, Prasad T, Ernst JF, Prasad R. 2005. Squalene epoxidase encoded by ERG1 affects morphogenesis and drug susceptibilities of *Candida albicans*. *Journal of Antimicrobial Chemotherapy*, 55(6):905–913.
- Pathania S, Rudramurthy SM, Narang T, Saikia UN, Dogra S. 2018. A prospective study of the epidemiological and clinical patterns of recurrent dermatophytosis at a tertiary care hospital in India. *Indian Journal of Dermatology, Venereology and Leprology*, 84(6):678–684.
- Peres NT, Sanches PR, Falco JP, Silveira HC, Paião FG, Maranhão FC, Gras DE, Segato F, Cazzaniga RA, Mazucato M, et al. 2010. Transcriptional profiling reveals the expression of novel genes in response to various stimuli in the human dermatophyte *Trichophyton rubrum*. *BMC Microbiology*, 10(1):1–10.
- Petrucelli MF, Matsuda JB, Peroni K, Sanches PR, Silva WA, Belebony RO, Martinez-Rossi NM, Marins M, Fachin AL. 2019. The transcriptional profile of *trichophyton rubrum* co-cultured with human keratinocytes shows new insights about gene modulation by terbinafine. *Pathogens*, 8(4).
- Pires RH, Martinez LR, Mendes-Giannini MJS, Stoianoff MAR. 2021. Editorial: Pathogenesis of Fungal Biofilms in Different Environmental Conditions and Clinical Outcomes. *Frontiers in Cellular and Infection Microbiology*, 11:1.
- Rezaei-Matehkolaei A, Khodavaisy S, Alshahni MM, Tamura T, Satoh K, Abastabar M, Shokoohi GR, Ahmadi B, Kord M, Taghipour S, et al. 2018. In vitro antifungal activity of novel triazole efinaconazole and five comparators against dermatophyte isolates. *Antimicrobial Agents and Chemotherapy*, 62(5).
- Rudramurthy SM, Shankarnarayan SA, Dogra S, Shaw D, Mushtaq K, Paul RA, Narang T, Chakrabarti A. 2018. Mutation in the squalene epoxidase gene of *trichophyton interdigitale* and *trichophyton rubrum* associated with allylamine resistance. *Antimicrobial Agents and Chemotherapy*, 62(5).

- Sacheli R, Harag S, Dehavay F, Evrard S, Rousseaux D, Adjetey A, Seidel L, Laffineur K, Lagrou K, Hayette MP. 2020. Belgian national survey on tinea capitis: Epidemiological considerations and highlight of terbinafine-resistant *T. mentagrophytes* with a mutation on SQLE gene. *Journal of Fungi*, 6(4):1–14.
- Salehi Z, Shams-Ghahfarokhi M, Razzaghi-Abyaneh M. 2018. Antifungal drug susceptibility profile of clinically important dermatophytes and determination of point mutations in terbinafine-resistant isolates. *European Journal of Clinical Microbiology and Infectious Diseases*, 37(10):1841–1846.
- Sanati H, Belanger P, Fratti R, Ghannoum M. 1997. A new triazole, voriconazole (UK-109,496), blocks sterol biosynthesis in *Candida albicans* and *Candida krusei*. *Antimicrobial Agents and Chemotherapy*, 41(11):2492–2496.
- Sanglard D. 2016. Emerging threats in antifungal-resistant fungal pathogens. *Frontiers in Medicine*, 3(MAR):1.
- Santos HL, Lang EAS, Segato F, Rossi A, Martinez-Rossi NM. 2018. Terbinafine resistance conferred by multiple copies of the salicylate 1-monooxygenase gene in *Trichophyton rubrum*. *Medical Mycology*, 56(3):378–381.
- Sardana K, Mathachan SR. 2021. Super Bioavailable Itraconazole and Its Place and Relevance in Recalcitrant Dermatophytosis: Revisiting Skin Levels of Itraconazole and Minimum Inhibitory Concentration Data. *Indian dermatology online journal*, 12(1):1–5.
- Sardana K, Gupta A, Sadhasivam S, Gautam RK, Khurana A, Saini S, Gupta S, Ghosh S. 2021. Checkerboard Analysis To Evaluate Synergistic Combinations of Existing Antifungal Drugs and Propylene Glycol Monocaprylate in Isolates from Recalcitrant Tinea Corporis and Cruris Patients Harboring Squalene Epoxidase Gene Mutation. *Antimicrobial agents and chemotherapy*, 65(8).
- Saunte DML, Hare RK, Jørgensen KM, Jørgensen R, Deleuran M, Zachariae CO, Thomsen SF, Bjørnskov-Halkier L, Kofoed K, Arendrup MC. 2019. Emerging terbinafine resistance in *Trichophyton*: Clinical characteristics, squalene epoxidase gene mutations, and a reliable EUCAST method for detection. *Antimicrobial Agents and Chemotherapy*, 63(10).

- Saunte DML, Pereiro-Ferreirós M, Rodríguez-Cerdeira C, Sergeev AY, Arabatzis M, Prohić A, Piraccini BM, Lecerf P, Nenoff P, Kotrekova LP, et al. 2021. Emerging antifungal treatment failure of dermatophytosis in Europe: take care or it may become endemic. *Journal of the European Academy of Dermatology and Venereology*.
- Seebacher C. 2003. Action mechanisms of modern antifungal agents and resulting problems in the management of onychomycosis. *Mycoses*, 46(11–12):506–510.
- Selmecki A, Forche A, Berman J. 2006. Aneuploidy and isochromosome formation in drug-resistant *Candida albicans*. *Science*, 313(5785):367–370.
- Shankarnarayan SA, Shaw D, Sharma A, Chakrabarti A, Dogra S, Kumaran MS, Kaur H, Ghosh A, Rudramurthy SM. 2020. Rapid detection of terbinafine resistance in *Trichophyton* species by Amplified refractory mutation system-polymerase chain reaction. *Scientific Reports*, 10(1).
- Shaw D, Singh S, Dogra S, Jayaraman J, Bhat R, Panda S, Chakrabarti A, Anjum N, Chowdappa A, Nagamoti M, et al. 2020. MIC and upper limit of wild-type distribution for 13 antifungal agents against a *Trichophyton mentagrophytes* *Trichophyton interdigitale* complex of Indian origin. *Antimicrobial Agents and Chemotherapy*, 64(4).
- Shukla PK, Singh P, Yadav RK, Pandey S, Bhunia SS. 2018. Past, present, and future of antifungal drug development. *Topics in Medicinal Chemistry*. 125–167, Springer Verlag;
- Singh A, Masih A, Khurana A, Singh PK, Gupta M, Hagen F, Meis JF, Chowdhary A. 2018. High terbinafine resistance in *Trichophyton interdigitale* isolates in Delhi, India harbouring mutations in the squalene epoxidase gene. *Mycoses*, 61(7):477–484.
- Singh A, Masih A, Monroy-Nieto J, Singh PK, Bowers J, Travis J, Khurana A, Engelthaler DM, Meis JF, Chowdhary A. 2019. A unique multidrug-resistant clonal *Trichophyton* population distinct from *Trichophyton mentagrophytes*/*Trichophyton interdigitale* complex causing an ongoing alarming dermatophytosis outbreak in India: Genomic insights and resistance profile. *Fungal Genetics and Biology*, 133.

- Singh A, Singh P, Dingemans G, Meis JF, Chowdhary A. 2021. Evaluation of Derma Genius® Resistance Real-Time Polymerase Chain Reaction (RT-PCR) for Rapid Detection of Terbinafine Resistant Trichophyton species. *Mycoses*.
- Siopi M, Efstathiou I, Theodoropoulos K, Pournaras S, Meletiadis J. 2021. Molecular Epidemiology and Antifungal Susceptibility of Trichophyton Isolates in Greece: Emergence of Terbinafine-Resistant Trichophytonmentagrophytes Type VIII Locally and Globally. *Journal of Fungi*, 7(6):419.
- Song J, Zhang S, Lu L. 2018. Fungal cytochrome P450 protein Cyp51: What we can learn from its evolution, regulons and Cyp51-based azole resistance. *Fungal Biology Reviews*, 32(3):131–142.
- Spettel K, Barousch W, Makristathis A, Zeller I, Nehr M, Selitsch B, Lackner M, Rath PM, Steinmann J, Willinger B. 2019. Analysis of antifungal resistance genes in *Candida albicans* and *Candida glabrata* using next generation sequencing. *PLoS ONE*, 14(1).
- Spettel K, Galazka S, Kriz R, Camp I, Willinger B. 2021. Do candida albicans isolates with borderline resistant micafungin mics always harbor fks1 hot spot mutations? *Journal of Fungi*, 7(2):1–7.
- Süß A, Uhrlaß S, Ludes A, Verma SB, Monod M, Krüger C, Nenoff P. 2019. Extensive tinea corporis due to a terbinafine-resistant Trichophyton mentagrophytes isolate of the Indian genotype in a young infant from Bahrain in Germany. *Hautarzt*, 70(11):888–896.
- Tabart J, Baldo A, Vermout S, Nusgens B, Lapiere C, Losson B, Mignon B. 2007. Reconstructed interfollicular feline epidermis as a model for *Microsporum canis* dermatophytosis. *Journal of medical microbiology*, 56(Pt 7):971–975.
- Tabart J, Baldo A, Vermout S, Losson B, Mignon B. 2008. Reconstructed interfollicular feline epidermis as a model for the screening of antifungal drugs against *Microsporum canis*. *Veterinary Dermatology*, 19(3):130–133.
- Taghipour S, Shamsizadeh F, Pchelin IM, Rezaei-Matehkolaei A, Mahmoudabadi AZ, Valadan R, Ansari S, Katirae F, Pakshir K, Zomorodian K, et al. 2020. Emergence of

- terbinafine resistant trichophyton mentagrophytes in iran, harboring mutations in the squalene epoxidase (Sqle) gene. *Infection and Drug Resistance*, 13:845–850.
- Tang C, Kong X, Ahmed SA, Thakur R, Chowdhary A, Nenoff P, Uhrlass S, Verma SB, Meis JF, Kandemir H, et al. 2021. Taxonomy of the Trichophyton mentagrophytes/T. interdigitale Species Complex Harboring the Highly Virulent, Multiresistant Genotype T. indotineae. *Mycopathologia*, 186(3):315–326.
- Tsai HF, Bard M, Izumikawa K, Krol AA, Sturm AM, Culbertson NT, Pierson CA, Bennett JE. 2004. *Candida glabrata* erg1 mutant with increased sensitivity to azoles and to low oxygen tension. *Antimicrobial Agents and Chemotherapy*, 48(7):2483–2489.
- Turenne CY, Sanche SE, Hoban DJ, Karlowsky JA, Kabani AM. 1999. Rapid identification of fungi by using the ITS2 genetic region and an automated fluorescent capillary electrophoresis system. *Journal of Clinical Microbiology*, 37(6):1846–1851.
- Vandeputte P, Ferrari S, Coste AT. 2012. Antifungal resistance and new strategies to control fungal infections. *International Journal of Microbiology*, 2012.
- Venkateswarlu K, Kelly DE, Manning NJ, Kelly SL. 1998. NADPH cytochrome P-450 oxidoreductase and susceptibility to ketoconazole. *Antimicrobial Agents and Chemotherapy*, 42(7):1756–1761.
- Verma S, Ramamoorthy R, Resham JV. 2022. Chronic eczema developing over skin treated for dermatophytosis in atopic patients -Importance of treating gently and intelligently. *Indian Journal of Dermatology*, 67(1):93.
- Verma SB, Panda S, Nenoff P, Singal A, Rudramurthy SM, Uhrlass S, Das A, Bisherwal K, Shaw D, Vasani R. 2021a. The unprecedented epidemic-like scenario of dermatophytosis in India: III. Antifungal resistance and treatment options. *Indian Journal of Dermatology, Venereology and Leprology*, 0:1.
- Verma SB, Panda S, Nenoff P, Singal A, Rudramurthy SM, Uhrlass S, Das A, Bisherwal K, Shaw D, Vasani R. 2021b. The unprecedented epidemic-like scenario of dermatophytosis in India: II. Diagnostic methods and taxonomical aspects. *Indian Journal of Dermatology, Venereology and Leprology*, 87(3):326–332.

- Verma SB, Panda S, Nenoff P, Singal A, Rudramurthy SM, Uhrlass S, Das A, Bisherwal K, Shaw D, Vasani R. 2021c. The unprecedented epidemic-like scenario of dermatophytosis in India: I. Epidemiology, risk factors and clinical features. *Indian Journal of Dermatology, Venereology and Leprology*, 87(2):154–175.
- White T, Bruns T, Lee S, Taylor J. 1990. Amplification and Direct Sequencing of Fungal Ribosomal RNA Genes for Phylogenetics. *PCR - Protocols and Applications - A Laboratory Manual*. 315–322, Academic Press, Inc.;
- White TC, Marr KA, Bowden RA. 1998. Clinical, cellular, and molecular factors that contribute to antifungal drug resistance. *Clinical Microbiology Reviews*, 11(2):382–402.
- Yamada T, Maeda M, Alshahni MM, Tanaka R, Yaguchi T, Bontems O, Salamin K, Fratti M, Monod M. 2017. Terbinafine resistance of Trichophyton clinical isolates caused by specific point mutations in the squalene epoxidase gene. *Antimicrobial Agents and Chemotherapy*, 61(7).
- Yazdanparast S, Barton R. 2006. Arthroconidia production in *Trichophyton rubrum* and a new ex vivo model of onychomycosis. *Journal of medical microbiology*, 55(Pt 11):1577–1581.
- Yu L, Zhang W, Wang L, Yang J, Liu T, Peng J, Leng W, Chen L, Li R, Jin Q. 2007. Transcriptional profiles of the response to ketoconazole and amphotericin B in *Trichophyton rubrum*. *Antimicrobial Agents and Chemotherapy*, 51(1):144–153.
- Zhang J, Li L, Lv Q, Yan L, Wang Y, Jiang Y. 2019. The fungal CYP51s: Their functions, structures, related drug resistance, and inhibitors. *Frontiers in Microbiology*, 10:691.
- Zhang W, Yu L, Yang J, Wang L, Peng J, Jin Q. 2009. Transcriptional profiles of response to terbinafine in *Trichophyton rubrum*. *Applied Microbiology and Biotechnology*, 82(6):1123–1130.